

General Disclaimer

One or more of the Following Statements may affect this Document

- This document has been reproduced from the best copy furnished by the organizational source. It is being released in the interest of making available as much information as possible.
- This document may contain data, which exceeds the sheet parameters. It was furnished in this condition by the organizational source and is the best copy available.
- This document may contain tone-on-tone or color graphs, charts and/or pictures, which have been reproduced in black and white.
- This document is paginated as submitted by the original source.
- Portions of this document are not fully legible due to the historical nature of some of the material. However, it is the best reproduction available from the original submission.

(NASA-TM-86172) RECENT EXAMPLES OF
MESOSCALE NUMERICAL FORECASTS OF SEVERE
WEATHER EVENTS ALONG THE EAST COAST (NASA)
66 p HC A04/MF A01 CSCL 04B

N85-12523

Unclas
G3/47 24515



Technical Memorandum 86172

RECENT EXAMPLES OF MESOSCALE NUMERICAL FORECASTS OF SEVERE WEATHER EVENTS ALONG THE EAST COAST

**Paul J. Kocin, Louis W. Uccellini,
John W. Zack, and Michael L. Kaplan**

NOVEMBER 1984

National Aeronautics and
Space Administration

Goddard Space Flight Center
Greenbelt, Maryland 20771

RECENT EXAMPLES OF MESOSCALE
NUMERICAL FORECASTS OF
SEVERE WEATHER EVENTS
ALONG THE EAST COAST

Paul J. Kocin¹, Louis W. Uccellini¹,
John W. Zack², and Michael L. Kaplan²

¹Goddard Laboratory for Atmospheres
NASA/Goddard Space Flight Center
Greenbelt, MD 20771

²Systems and Applied Sciences Corporation
Hampton, VA 23666

ABSTRACT

Mesoscale numerical forecasts utilizing the Mesoscale Atmospheric Simulation System (MASS) are documented for two East Coast severe weather events. The two events are the thunderstorm and heavy snow bursts in the Washington, DC-Baltimore, MD region on 8 March 1984 and the devastating tornado outbreak across North and South Carolina on 28 March 1984. The forecasts are presented to demonstrate the ability of the model to simulate dynamical interactions and diabatic processes and to note some of the problems encountered when using mesoscale models for day-to-day forecasting.

CONTENTS

	<u>Page</u>
1. INTRODUCTION	1
2. A SUMMARY OF MASS: ITS RECENT USE AND EVALUATION	3
3. THE 8 MARCH 1984 WASHINGTON, DC-BALTIMORE, MD THUNDER/SNOW BURST	9
a. Surface and Weather Analyses	9
b. Model Forecast of Sea-Level Pressure and Pressure Tendency	15
c. Model Forecast of Upper-Level Fields	19
d. Model Forecast of 700 mb Vertical Motions, Lifted Index and Precipitation Amounts	23
e. Model Forecast of the Rain-Snow Line	27
f. Summary of the 8 March 1984 MASS Simulation	28
4. THE 28 MARCH 1984 NORTH AND SOUTH CAROLINA TORNADO OUTBREAK . .	29
a. Surface and Weather Analyses	29
b. Model Forecast of Sea-Level Pressure and Pressure Tendency	35
c. Model Forecast of Upper-Level Fields	38
d. Model Forecast of 700 mb Vertical Motions, Lifted Index and Precipitation Amounts	43
e. Summary of the 28 March 1984 MASS Simulation	45
5. SUMMARY	49
Acknowledgements	51
REFERENCES	53

LIST OF FIGURES

Page

- Figure 1. Sea-level pressure (mb) and surface frontal analyses for 1200 GMT 8 March, 1800 GMT 8 March, and 0000 GMT 9 March 1984. Shading represents precipitation occurring at the time of the analysis. 10
- Figure 2. Total snowfall (cm) and hourly series of selected surface weather reports for 8 March 1984 for the region surrounding and including Washington, DC and Baltimore, MD. Hourly series are shown for Dulles International Airport (IAD), Washington National Airport (DCA), and Baltimore-Washington International Airport (BWI), and include temperature ($^{\circ}\text{C}$), current weather conditions (symbols standard), and sea-level pressure (108 = 1010.8 mb). Snowfall measurements were taken from official National Weather Service observations, a local reporting group from the NASA/Goddard Space Flight Center, Greenbelt, MD, and the Metropolitan Washington Climate Review for March 1984. T represents trace amounts. 12
- Figure 3. Three-hourly SMS-GOES infrared satellite imagery between 1200 GMT 8 March and 0300 GMT 9 March 1984. Figure includes surface low positions and c refers to the expanding region of colder cloud-top temperatures between 1800 GMT 8 March and 0000 GMT 9 March 1984. 14
- Figure 4. LFM initial analysis at 1200 GMT 8 March 1984 and 12 h LFM forecasts verifying at 0000 GMT 9 March 1984. (a) 1200 GMT 8 March initial analysis and (b) 12 h surface forecast include sea-level isobars (solid, 20 = 1020 mb) and 1000 to 500 mb thickness contours (dashed, 540 = 5400 m). (c) 12 h forecast 700 mb heights (solid, 300 = 3000 m) and mean relative humidities through the three lowest sigma layers (dashed; 5 = 50%; shading for humidities in excess of 70%). (d) 12 h forecast 700 mb vertical motions (dashed; +4 = $-4 \mu\text{b s}^{-1}$) and 12 h accumulated precipitation (shaded; 047 = 0.47 in). 16
- Figure 5. Three-hourly surface analyses and MASS forecasts between 1500 GMT 8 March and 0000 GMT 9 March 1984 from model initialized at 1200 GMT 8 March 1984. The surface analyses include station reports of weather type and air temperature ($^{\circ}\text{C}$), isobars (in increments of 4 mb), fronts, wind barbs (each full barb represents 5 m s^{-1} ; each half barb represents 2.5 m s^{-1}), precipitation occurring at the time of the analysis (shading), and isotherms (dashed, 0°C and 10°C). The

sea-level pressure forecast includes isobars (solid, in increments of 4 mb), and forecast isotherms (dashed, 0°C and 10°C) in the lowest model layer. The thick solid line in the pressure tendency forecast [$-2.3 = -2.3 \text{ mb (3 h)}^{-1}$] separates three-hourly predicted positive and negative pressure tendencies.

18

Figure 6. Three-hourly MASS forecasts of selected 300 mb, 500 mb, and 850 mb fields between 1800 GMT 8 March and 0000 GMT 9 March 1984 from model initialized at 1200 GMT 8 March 1984. Verifying analyses at 0000 GMT 9 March are located at the bottom of the figure. The left-hand column includes 500 mb heights (solid, 540 = 5400 m), absolute vorticity (thin-dashed; x's denote vorticity maxima; $29.7 = 29.7 \times 10^{-5} \text{ s}^{-1}$), and locations of 300 mb jet maxima (denoted by a J; $65 = 65 \text{ m s}^{-1}$). Vorticity analysis at 0000 GMT 9 March taken from LFM analysis. The middle column includes 850 mb heights (solid, 138 = 1380 m) and isotherms (dashed, $^{\circ}\text{C}$). The right-hand column (forecasts only) includes 850 mb wind vectors and isotachs (solid, m s^{-1}). Observed winds (bottom right) feature wind barbs (each barb represents 5 m s^{-1} ; each half barb represents 2.5 m s^{-1} ; M denotes missing observations).

20

Figure 7. Three-hourly MASS forecasts of 700 mb vertical motion ($-12.7 = -12.7 \mu\text{b s}^{-1}$; thick solid line separates ascent and descent), lifted index (thick solid lines are in increments of 2 for values less than 4; shading is for values less than 0), and three-hourly accumulated stable (solid contours) and convective (shaded regions) precipitation ($25 = 0.25 \text{ cm}$) between 1500 GMT 8 March and 0000 GMT 9 March 1984 from model initialized at 1200 GMT 8 March 1984.

24

Figure 8. Tornado paths and times of occurrences (GMT) (from March 1984 Storm Data) between 2100 GMT 28 March 1984 and 0300 GMT 29 March 1984.

30

Figure 9. Sea-level pressure (mb) and surface frontal analyses for 1800 GMT 28 March, 0000 GMT 29 March, and 0600 GMT 29 March 1984. Shading represents precipitation occurring at the time of the analysis.

32

Figure 10. Selected SMS-GOES infrared satellite imagery between 1800 GMT 28 March and 0330 GMT 29 March 1984, which covers the period of the Carolinas tornado outbreak. Figure includes surface low positions and c refers to the expanding region of colder cloud top temperatures.

34

Figure 11. Three-hourly surface analyses and MASS forecasts between 1800 GMT 28 March and 0300 GMT 29 March 1984

from model initialized at 1200 GMT 28 March 1984. See Fig. 5 for additional details. Note that isotherm analysis and forecast is not included here.

36

Figure 12. Analysis and 12 h MASS and LFM forecasts of sea-level pressure at 0000 GMT 29 March 1984.

39

Figure 13. Three-hourly MASS forecasts of selected 300 mb, 500 mb, and 850 mb fields between 1800 GMT 28 March and 0300 GMT 29 March 1984 from model initialized at 1200 GMT 28 March 1984. The verifying analyses at 0000 GMT 29 March 1984 appear immediately below the 0000 GMT forecasts. See Fig. 6 for additional details.

40

Figure 14. Three-hourly MASS forecasts of 700 mb vertical motion ($-11.4 = -11.4 \mu b s^{-1}$; thick solid lines separate ascent and descent). Lifted index (thick solid lines are in increments of 4 for values less than 0; shading is for values less than -4), and three-hourly accumulated convective precipitation ($25 = 0.25 \text{ cm}$) between 1800 GMT 28 March and 0300 GMT 29 March 1984 from model initialized at 1200 GMT 28 March 1984.

44

Figure 15. Analysis of 300 mb height (thick solid, 900 = 9000 m) and wind speed (thin solid, $m s^{-1}$) for 1200 GMT 28 March 1984. Flags represent speeds of $25 m s^{-1}$; barbs represent speeds of $5 m s^{-1}$; half barbs represent $2.5 m s^{-1}$ speeds. M denotes missing wind reports.

47

LIST OF TABLES

	<u>Page</u>
Table 1. Basic characteristics of MASS 3.0 (June 1983).	4
Table 2. List of MASS model simulations used for case studies.	5

1. INTRODUCTION

Recent advances in high-speed computers have facilitated the development of mesoscale numerical models that can be run in real-time and produce detailed mesoscale forecasts for large domains. One such modeling system is named the Mesoscale Atmospheric Simulation System (MASS), located at the NASA/Langley Research Center (LRC) in Hampton, Virginia. Synoptic and mesoscale forecasts from an earlier version of MASS have been evaluated for a large number of cases (Koch, 1984; Koch et al., 1984). The model has also been applied to detailed diagnostic studies of spring and summer severe convective storm systems (e.g., Zack, 1981; Kaplan et al., 1984) and East Coast winter storm systems (Kaplan et al., 1982a; Uccellini et al., 1983; Zack et al., 1984). The ability of mesoscale models, such as MASS, to improve upon current operational model forecasts is based on such factors as increased horizontal and vertical resolution, inclusion of significant level data for initialization, inclusion of cumulus parameterization schemes, and more complex planetary boundary layer formulations which involve explicit prediction of the heights of the boundary layer and the use of a soil moisture budget.

The purpose of this paper is to review two recent examples of model forecasts of severe weather events along the East Coast made with an updated version of MASS initialized with the operational rawinsonde data base. The first case is the 8 March 1984 thunder/snow burst which produced up to 15 cm of snow in the northern suburbs of Washington, DC and throughout the Baltimore metropolitan area in only 1 to 3 h during the evening rush hour. The intensity and amount of snow was not predicted by

the LFM model nor by any of the local weather services. The second case is the 28 March 1984 tornado outbreak that devastated portions of North and South Carolina. The review of the model performance for these cases, however, is not meant to be a quantitative evaluation, as was done by Koch (1984) and Koch et al. (1984). Rather, the goal of this paper is to illustrate that useful mesoscale forecasts can be generated for East Coast severe storm systems and to note several difficult problems encountered when using mesoscale models for routine, short-range forecasting. The version of MASS used for the March 1984 cases is briefly reviewed in Section 2. The model forecasts for 8 March and 28 March 1984 are presented in Sections 3 and 4, respectively. The results are summarized in Section 5.

2. A SUMMARY OF MASS: ITS RECENT USE AND EVALUATION

MASS is based on a fourteen-layer primitive equation model that is typically run over a domain that covers most of North America [see Kaplan et al. (1982b, p. 1566)], but is smaller than that used for the National Meteorological Center's (NMC's) Limited Area Fine Mesh model (LFM). The model has twice the vertical resolution of the LFM and a smaller grid increment of 47.6 km true at 40°N on a polar stereographic projection. The simulation system is described by Kaplan et al. (1982b), with more recent modifications described by Wong et al. (1983a, b). The basic components of the model used here, including the planetary boundary layer formulation and cumulus parameterization scheme, are listed in Table 1. An important aspect of MASS is that the data required to initialize the model temperature, wind, and moisture fields can be accessed and archived in real-time via a 4800 baud telephone line between NASA/LRC and the Water and Power Resources Service Data Base in Denver, CO. This initial data configuration includes the LFM analysis, LFM forecasts, mandatory and significant level rawinsonde data, and hourly surface observations. The LFM analysis serves as a first guess field over the entire model domain for a Cressman (1959) analysis scheme that incorporates the significant level rawinsonde and hourly surface data sets. The LFM forecasts are used to specify time-dependent boundary conditions for the MASS simulations.

The incorporation of real-time data into the front end of MASS has allowed the use of the meso- α -scale model for simulating a large number and variety of severe weather events across the United States, including many examples of mesoscale convective systems and intense coastal and

Table 1

Basic Characteristics of MASS 3.0 (June 1983)

- 1) A matrix of 128 by 96 grid points with a horizontal grid increment \approx 47.6 km true at 40°N on a polar stereographic projection covering most of North America and adjacent waters.
- 2) 14 layers in a sigma-p coordinate system.
- 3) Nested grid capability to \approx 14 km.
- 4) Euler-backward time marching.
- 5) Fourth-order accurate space differencing.
- 6) Generalized similarity theory planetary boundary layer with a surface temperature and moisture budget, as well as time-dependent equations for the PBL height.
- 7) A choice of cumulus parameterization schemes (Anthes, 1977; Fritsch and Chappell, 1980; Molinari, 1982). The Anthes (1977) scheme was used for the model simulations described in this paper.
- 8) Grid-scale stable latent heating.
- 9) Dry convective adjustment.
- 10) Time-dependent boundary conditions based on LFM forecast.
- 11) Static initialization scheme.
- 12) LFM analysis, mandatory and significant level rawinsonde, and hourly surface data sets used to initialize the model.
- 13) Soil characteristics, sea surface temperature, ground wetness, albedo, and vegetative cover accounted for in surface energy budget.

Table 2

List of MASS Model Simulations Used for Case Studies

Date	Version of MASS	Type of System	References
18-19 February 1979	2.0, 3.0	Mid-Atlantic states snowstorm ("Presidents' Day" snowstorm)	<u>Uccellini et al.</u> (1983)
10-11 April 1979	1.0, 2.0, 3.0	Red River Valley, TX and OK Tornado Outbreak	<u>Zack</u> (1981), <u>Kaplan et al.</u> (1982b, c, d)
3-4 October 1979	1.0	Windsor Locks, CT Tornado Outbreak	----
12-13 May 1980	1.0	Sedalia, MO Tornado Outbreak	----
3-4 June 1980	1.0, 2.0, 3.0	Grand Island, NE Tornado Outbreak	<u>Wong</u> (1982), <u>Zack et al.</u> (1983), <u>Kaplan et al.</u> (1984), <u>Coats et al.</u> (1984)
3-4 April 1981	1.0	West Bend, WI Tornado Outbreak (also date of the Hannibal, MO Aircraft Accident)	<u>Kaplan et al.</u> (1981)
20-21 July 1981	3.0	Illinois Severe Storm Outbreak (used for VAS impact study)	<u>Cram et al.</u> (1984)
12-13 October 1981	2.0	Breckenridge, TX Floods	----
2-3 April 1982	2.0, 3.0	Paris, TX Tornado Outbreak	<u>Wong et al.</u> (1983a, b), <u>Koch</u> (1984)
5-7 April 1982	2.0, 3.0	Record Breaking Snowstorm for Northeastern United States	<u>Kaplan et al.</u> (1982a)

13-14 April 1982	2.0	Isolated Severe Texas Storms	Koch (1984)
21, 25-27 June 1982	3.0	Florida Sea Breeze Convection Cases (includes Shuttle Hailstorm)	----
10-11 February 1983	3.0	Record Middle Atlantic Snowstorm	Zack <u>et al.</u> (1984)
22-23 April 1983	3.0	Flooding and Tornadoes in Southeastern United States	----
18-19 May 1983	3.0	Rocky Mountain Spring Blizzard	----
20-21 May 1983	3.0	Houston, TX Tornadoes and Flooding	----
23-24 June 1983	3.0	Florida Convection (Space Shuttle STS-7 landing)	----
29-30 August 1983	3.0	Florida Convection (Space Shuttle STS-8 liftoff)	----
20-21 April 1984	3.0	Mississippi Tornado Outbreak	----
26-27 April 1984	3.0	Tulsa, OK Flooding	----

continental cyclogenesis (see Table 2). These cases have been used to study a range of processes that play important roles in the development of storm systems, including (a) the interactions between jet streak circulations and boundary layer heating (Kaplan et al., 1984; Wong, 1982), (b) the interplay between jet streaks, air-sea interactions, and diabatic processes, all of which appear to influence East Coast snowstorms (Uccellini et al., 1983; Zick et al., 1984), and (c) the secondary redevelopment of cyclones along the East Coast of the United States (Kaplan et al., 1982a).

An early version of MASS (version 2.0) was evaluated at the NASA/Goddard Space Flight Center to determine the model's predictive skill and systematic errors (Koch, 1984; Koch et al., 1984). The evaluation was conducted in an objective (statistical) and subjective manner. Thirty model forecasts from the spring and summer of 1982 were examined and compared to output from NMC's LFM model to determine the synoptic-scale performance of MASS. MASS was also evaluated in terms of its ability to simulate the mesoscale environment preceding convection. The evaluation showed that although MASS 2.0 was outperformed by the LFM in forecasts of a few middle- and upper-tropospheric fields, it equaled or exceeded the LFM in synoptic-scale forecasts of nearly all fields after cases with systematic mass loss errors along the eastern boundary were deleted. It was also shown that MASS 2.0 forecasts provided coherent mesoscale fields useful for forecasting the initiation of convection. Finally, MASS 2.0 vertical motions were combined with other mesoscale forecast fields and produced "predictor variables," which were accurately related to the locus

of approximately half of the strong mesoscale convective systems observed during the three-month experiment.

The results of the evaluation have been used to further improve the model and to formulate MASS version 3.0. Improvements made to the modeling system since the evaluation was completed include a soil moisture budget (Deardorff, 1977), an improved time marching scheme for the surface energy budget (Bhumralker, 1975), a choice of cumulus parameterization schemes (Anthes, 1977; Fritsch and Chappell, 1980; Molinari, 1982), and a maritime planetary boundary layer formulation (Stage and Businger, 1981). Numerous model forecasts were conducted in real-time during the spring and summer of 1983 to test the refinements and additions to MASS 3.0.

The application of MASS 3.0 to the simulation of two East Coast severe weather events is described in the following sections. The first case involves an outbreak of intense snow-producing thunderstorms in the Washington, DC-Baltimore, MD metropolitan areas that was associated with a rapidly moving mid-latitude cyclone on 8 March 1984. The second case involves the major tornado outbreak across South and North Carolina that was associated with a large and unusually intense mid-latitude cyclone on 28 March 1984. The model simulations were run several days after the events because of financial constraints. However, no special changes or modifications were made to the data base received and archived at NASA/LRC. Furthermore, since the run-time for the 24 h forecast was only forty-five minutes, the computer-plotted model forecast and output products could have been available for forecasting purposes within approximately two hours from the time when the initial data were processed and transmitted.

3. THE 8 MARCH 1984 WASHINGTON, DC-BALTIMORE, MD THUNDER/SNOW BURST

a. Surface and Weather Analyses

The 8 March 1984 case is notable as a severe weather event in Washington, DC and Baltimore, MD as an area of unpredicted thunderstorms accompanied by excessive snowfall rates and near-zero visibilities paralyzed the region during the evening rush hour. Six-hourly surface maps derived from NMC analyses between 1200 GMT 8 March and 0000 GMT 9 March are shown in Fig. 1 to describe the synoptic setting for the convective snow event. At 1200 GMT 8 March, a small, but well-defined, surface low pressure center with a central pressure of 1007 mb was located over central Indiana. A cold front trailed southward from the low into Tennessee and then southwestward into Texas. A warm front was located across eastern Kentucky into southern Virginia. A band of moderate to occasionally heavy snow was falling immediately north and east of the low center with 7 to 10 cm accumulations over a 6 to 12 h period across the northern Ohio Valley. A high over southern Manitoba was accompanied by unusually cold temperatures for early March and possessed two ridge axes; one extending south through the Plains states and the other extending east-southeastward into the northeastern United States. The low had little available moisture as high pressure and subsidence over the Gulf of Mexico effectively shut off that region as a moisture source.

By 1800 GMT, the surface low had progressed eastward to eastern Ohio as its central pressure remained constant at approximately 1007 mb. Heaviest snowfall continued to occur near the low center, with moderate to heavy snows falling across eastern Ohio, western Pennsylvania and northern

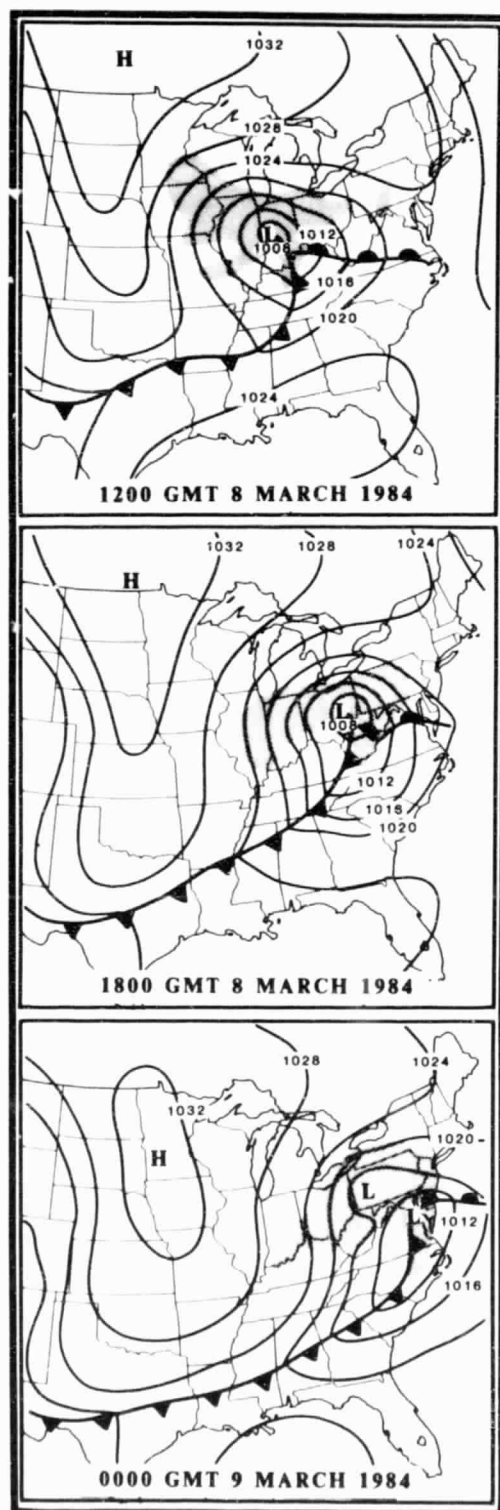


Figure 1. Sea-level pressure (mb) and surface frontal analyses for 1200 GMT 8 March, 1800 GMT 8 March, and 0000 GMT 9 March 1984. Shading represents precipitation occurring at the time of the analysis.

West Virginia, while light snows were advancing across western Maryland and southern Pennsylvania. The warm front had advanced into northern Virginia, with temperatures approaching 10°C in central Virginia while remaining near 0°C over central Maryland ahead of the front. As the low approached the Appalachian range, surface pressure falls were centered not only to the east of the low but also further southward over Virginia and North Carolina. Convection was reported over portions of West Virginia; Charleston, WV measured pea-size hail prior to 1800 GMT.

During the following 6 h, some subtle but important changes occurred. The surface low previously located over eastern Ohio drifted into western Pennsylvania, where it weakened. At the same time, a secondary low center formed to its south and east over central Virginia. The secondary low center moved rapidly northeastward to just south of Washington, DC by 0000 GMT. During this period, a region of intense convection developed over western Virginia and moved to the northeast. Heavy thunderstorms with snow falling at a rate approaching 10 to 12 cm h^{-1} spread across the northern suburbs of Washington and much of metropolitan Baltimore between 2100 and 0000 GMT, depositing up to 17 cm of snow in the region between the two cities (Fig. 2).

A series of hourly surface weather reports (Fig. 2) from the Washington-Baltimore area, including Dulles International Airport (IAD), Washington National Airport (DCA), and Baltimore-Washington International Airport (BWI), illustrates the widely varying weather conditions that preceded and accompanied the snow burst, as well as its progression through the region between 1800 GMT 8 March and 0000 GMT 9 March. Heavy snow developed at IAD by 2152 GMT and began at DCA and BWI at 2243 GMT and

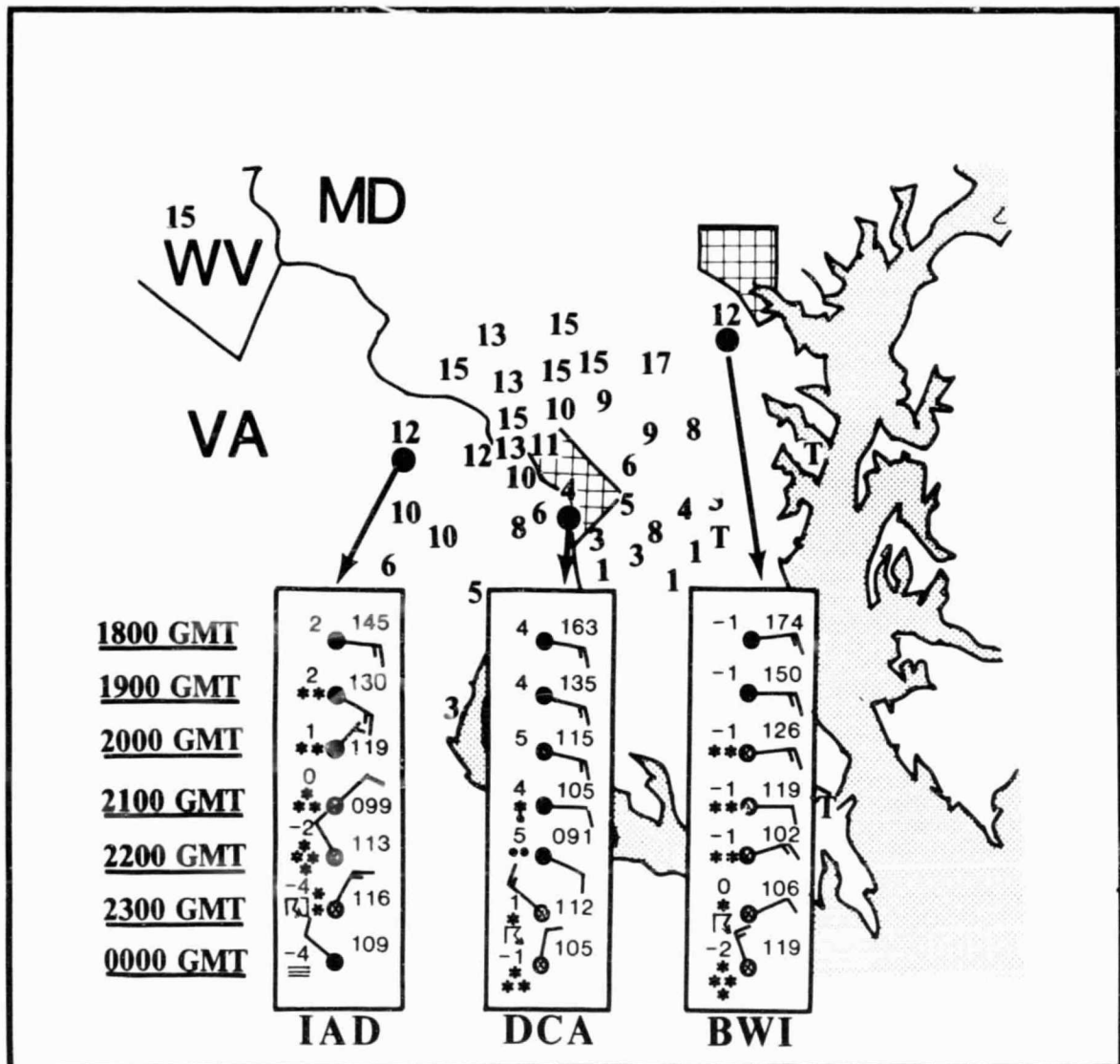


Figure 2. Total snowfall (cm) and hourly series of selected surface weather reports for 8 March 1984 for the region surrounding and including Washington, DC and Baltimore, MD. Hourly series are shown for Dulles Airport (IAD), Washington National Airport (DCA), and Baltimore-Washington International Airport (BWI), and include temperature ($^{\circ}\text{C}$), current weather conditions (symbols standard), and sea-level pressure (108 = 1010.8 mb). Snowfall measurements were taken from official National Weather Service observations, a local reporting group from the NASA/Goddard Space Flight Center, Greenbelt, MD, and the Metropolitan Washington Climate Review for March 1984. T represents trace amounts.

2324 GMT, respectively. Thunder and lightning were observed at all three airports. At the onset of the snow burst, local weather conditions varied considerably across the region. The 2200 GMT observations shown in Fig. 2 depict the mesoscale character of weather conditions prevailing across northern Virginia and central Maryland. At 2200 GMT, heavy snow, rising pressure, temperatures falling below -2°C , and northwesterly winds were recorded at IAD, while DCA was concurrently reporting light rain, falling pressure, a temperature of 5°C , and southeasterly winds. Before the evening was over, however, all locations in the immediate Washington-Baltimore area recorded heavy snow, lightning and thunder, visibilities near zero, a brief period of rapidly rising pressure, a shift to northwesterly winds, and a dramatic drop of temperature.

In the 24 h period following 0000 GMT 9 March, the surface low, which had re-formed in Virginia, continued moving northeastward into central Delaware and southern New Jersey and then over the Atlantic Ocean just south of Long Island. Heaviest snows fell in a narrow band immediately north of the low center with 18 cm at Philadelphia, 22 cm at New York City - LaGuardia Airport, and 35 cm at Nantucket, MA. Falling temperatures and gale force winds created near-blizzard conditions for a time on 9 March through coastal New Jersey, New York and southern New England.

A sequence of 3-hourly infrared GOES-East satellite images are presented in Fig. 3 to describe the cloud structure associated with the cyclone and to highlight the convective development that occurred over Virginia and Maryland. The infrared images between 1200 and 1800 GMT show a comma-shaped cloud pattern moving east from the Ohio Valley, with several distinct banded cloud features aligned generally from northeast to

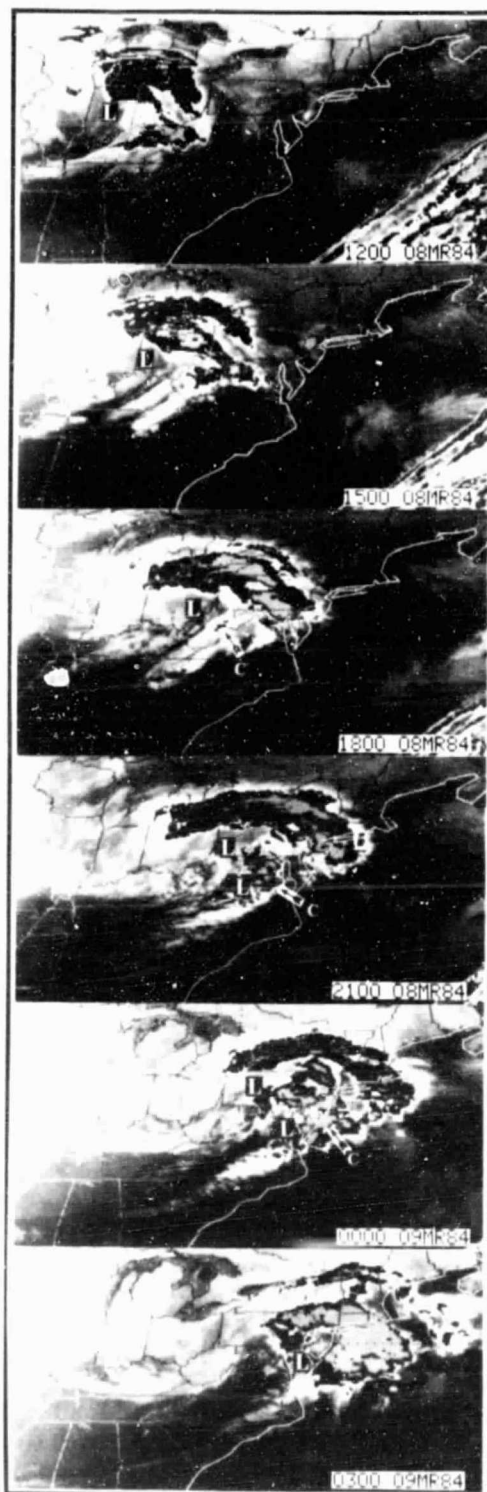


Figure 3. Three-hourly SMS-GOES infrared satellite imagery between 1200 GMT 8 March and 0300 GMT 9 March 1984. Figure includes surface low positions and c refers to the expanding region of colder cloud-top temperatures between 1800 GMT 8 March and 0000 GMT 9 March 1984.

southwest within the "tail" of the comma across Kentucky and West Virginia. As a region of cold cirrus cloud tops moved northeastward into Pennsylvania, a new cloud region (with colder cloud top temperatures) appeared across eastern West Virginia at 1800 GMT. This cloud system expanded greatly in size during the following 3 to 9 h as it moved toward the East Coast. The growth of this cloud mass at 2100 and 0000 GMT was accompanied by many reports of thunderstorms that produced the unpredicted heavy snow across Virginia and Maryland. This cloud mass was also later responsible for the heavy snow which fell across eastern Pennsylvania, New Jersey, New York City and southern New England on 9 March.

b. Model Forecast of Sea-Level Pressure and Pressure Tendency

A common difficulty inherent in cyclone prediction along the East Coast of the United States is the forecast of the location and timing of the secondary development of the surface low to the east of the Appalachian mountains. In this case, the rapid movement of the surface low from Ohio to near Washington, DC between 1200 GMT 8 March and 0000 GMT 9 March and the coarse resolution of the larger-scale LFM model forecast initialized at 1200 GMT 8 March (Fig. 4) prevented a clear forecast of whether, where, and when secondary development would occur for this case. Surface observations on the morning of 8 March indicated that the surface low was moving eastward across central Indiana and Ohio (Fig. 1). Both the LFM 12 h sea-level pressure forecast (Fig. 4) and an extrapolation of the movement of the surface low would have taken the low slightly north of the Washington, DC area by the evening of 8 March, making the region unfavorable for heavy snow (Browne and Younkin, 1970; Spiegler and Fisher,

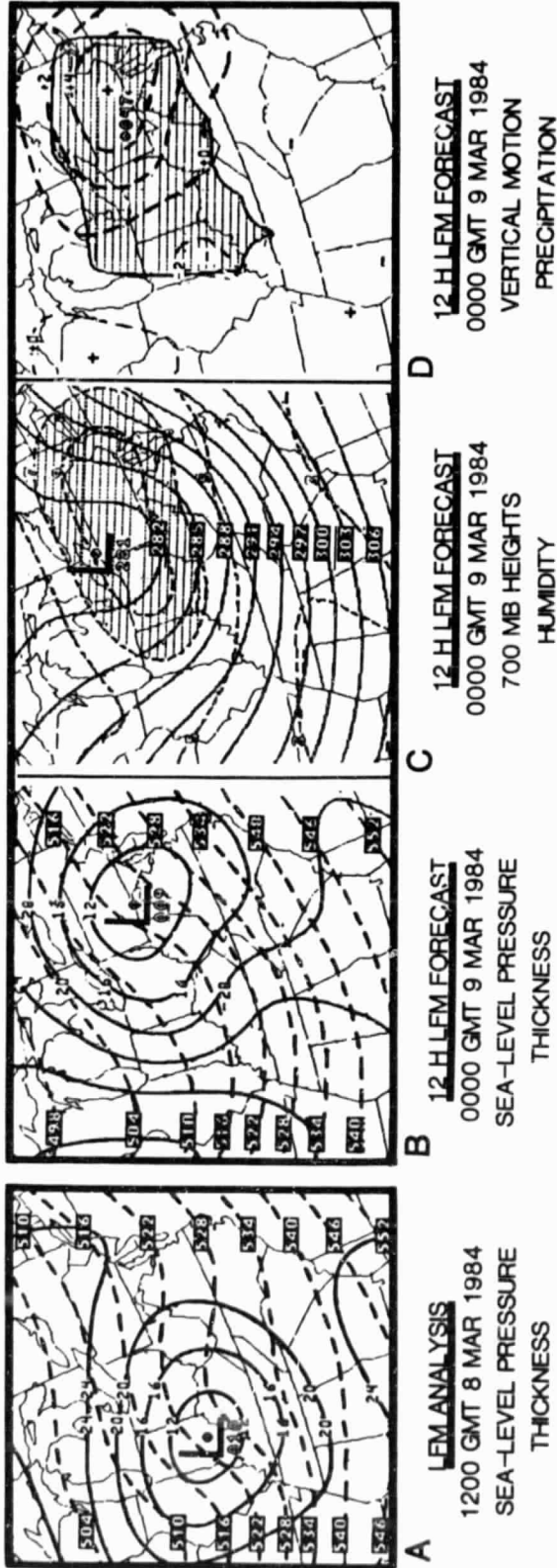


Figure 4. LFM initial analysis at 1200 GMT 8 March 1984 and 12 h LFM forecasts verifying at 0000 GMT 9 March 1984. (a) 1200 GMT 8 March initial analysis and (b) 12 h surface forecast include sea-level isobars (solid, 20 = 1020 mb) and 1000 to 500 mb thickness contours (dashed, 540 = 5400 m). (c) 12 h forecast 700 mb heights (solid, 300 = 3000 m) and mean relative humidities through the three lowest sigma layers (dashed; 5 = 50%; shading for humidities in excess of 70%). (d) 12 h forecast 700 mb vertical motions (dashed; +4 = $-4 \mu\text{b s}^{-1}$) and 12 h accumulated precipitation (shaded; 0.47 = 0.47 in).

1971). Local forecasters seemed assured that heavy snow amounts were likely across Pennsylvania, New Jersey, and southern New York, but hesitated in forecasting snow amounts in the Washington-Baltimore area, although the LFM 12 h 700 mb vertical motion and lower-tropospheric mean relative humidity forecasts (Fig. 4) placed the region at the southern limit of the maximum ascent and largest mean relative humidities. The consensus of local forecasters indicated the potential for accumulations of 2.5 to 5 cm at most.

In Figure 5, the MASS three-hourly sea-level pressure and pressure tendency simulations initialized at 1200 GMT 8 March are compared to observed analyses between 1500 GMT 8 March and 0000 GMT 9 March to assess the model forecast of the track, intensity and redevelopment of the surface low. The 3 h MASS simulation of sea-level pressure and pressure tendency valid at 1500 GMT 8 March is in good agreement with the analysis as the predicted low center is located near Cincinnati, OH. The 1800 GMT simulation places the surface low close to the observed surface low near the Ohio-West Virginia border, although the forecast central sea-level pressure is 3 mb too high. However, the model's surface pressure forecast also hints at redevelopment of the surface low across central and southern Virginia as the forecast low center is now slightly elongated from southeastern Ohio into southwestern Virginia. Further evidence of the model's suggestion of redevelopment to the southeast of the main low center is seen from the pressure tendency forecast at 1800 GMT. This forecast shows two separate pressure fall centers, one near the border of Pennsylvania, Maryland and West Virginia, and the other centered near the South and North Carolina border.

3-HOURLY SURFACE ANALYSES AND
MASS (3.0) FORECASTS
MODEL INITIALIZED AT 1200 GMT 8 MARCH 1984

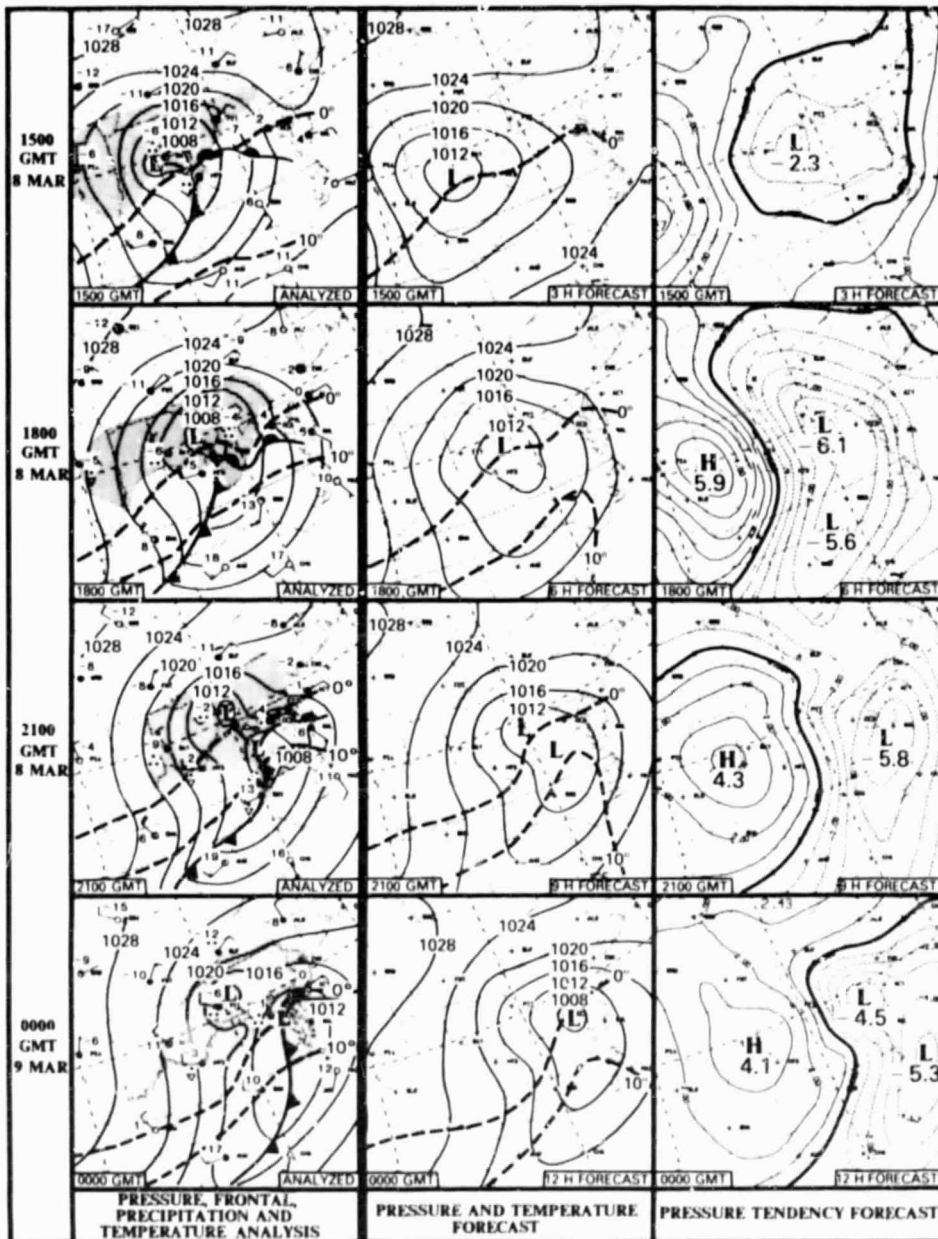


Figure 5. Three-hourly surface analyses and MASS forecasts between 1500 GMT 8 March and 0000 GMT 9 March 1984 from model initialized at 1200 GMT 8 March 1984. The surface analyses include station reports of weather type and air temperature ($^{\circ}\text{C}$), isobars (in increments of 4 mb), fronts, wind barbs (each full barb represents 5 m s^{-1} ; each half barb represents 2.5 m s^{-1}), precipitation occurring at the time of the analysis (shading), and isotherms (dashed, 0°C and 10°C). The sea-level pressure forecast includes isobars (solid, in increments of 4 mb), and forecast isotherms (dashed, 0°C and 10°C) in the lowest model layer. The thick solid line in the pressure tendency forecast [$-2.3 = -2.3 \text{ mb (3 h)}^{-1}$] separates three-hourly predicted positive and negative pressure tendencies.

By 2100 GMT, surface analyses indicated that a new low center had developed across central Virginia while the old low center had become more diffuse over southwestern Pennsylvania. The MASS simulation valid at 2100 GMT predicts a 1009 mb low center over west-central Virginia, approximately 300 km to the southeast of its location 3 h earlier. The forecast position of this new surface low matches almost exactly the observed position of the redeveloped center. The surface pressure tendency forecast for the period between 1800 and 2100 GMT indicates only one major elongated pressure fall center maximized over eastern Virginia. The model simulation for 0000 GMT 9 March forecasts the secondary low center to propagate northeastward and deepen slightly to 1007 mb just south and west of Washington, DC, a position slightly north and west of the actual location. To summarize, MASS not only captures the initial track of the primary low center, but also accurately predicts the timing and location of the redevelopment of the surface low east of the Appalachian Mountains for this case.

c. Model Forecast of Upper-Level Fields

MASS simulations of 500 mb geopotential height and absolute vorticity, 300 mb wind speed maxima, and 850 mb geopotential height, winds and temperatures at 1800 GMT 8 March through 0000 GMT 9 March are shown in Fig. 6. The MASS 12 h forecasts verifying at 0000 GMT 9 March are discussed first to benchmark the model performance against analyses derived from 0000 GMT rawinsonde observations.

The forecast location and amplitude of the 500 mb short wave trough at 0000 GMT is comparable to the analyzed trough, but the axis is perhaps 50

MASS (3.0) 3-HOURLY FORECASTS OF
SELECTED 300 MB, 500 MB AND 850 MB
FIELDS
MODEL INITIALIZED AT 1200 GMT 8 MARCH 1984
VERIFYING ANALYSES AT 0000 GMT 9 MARCH 1984

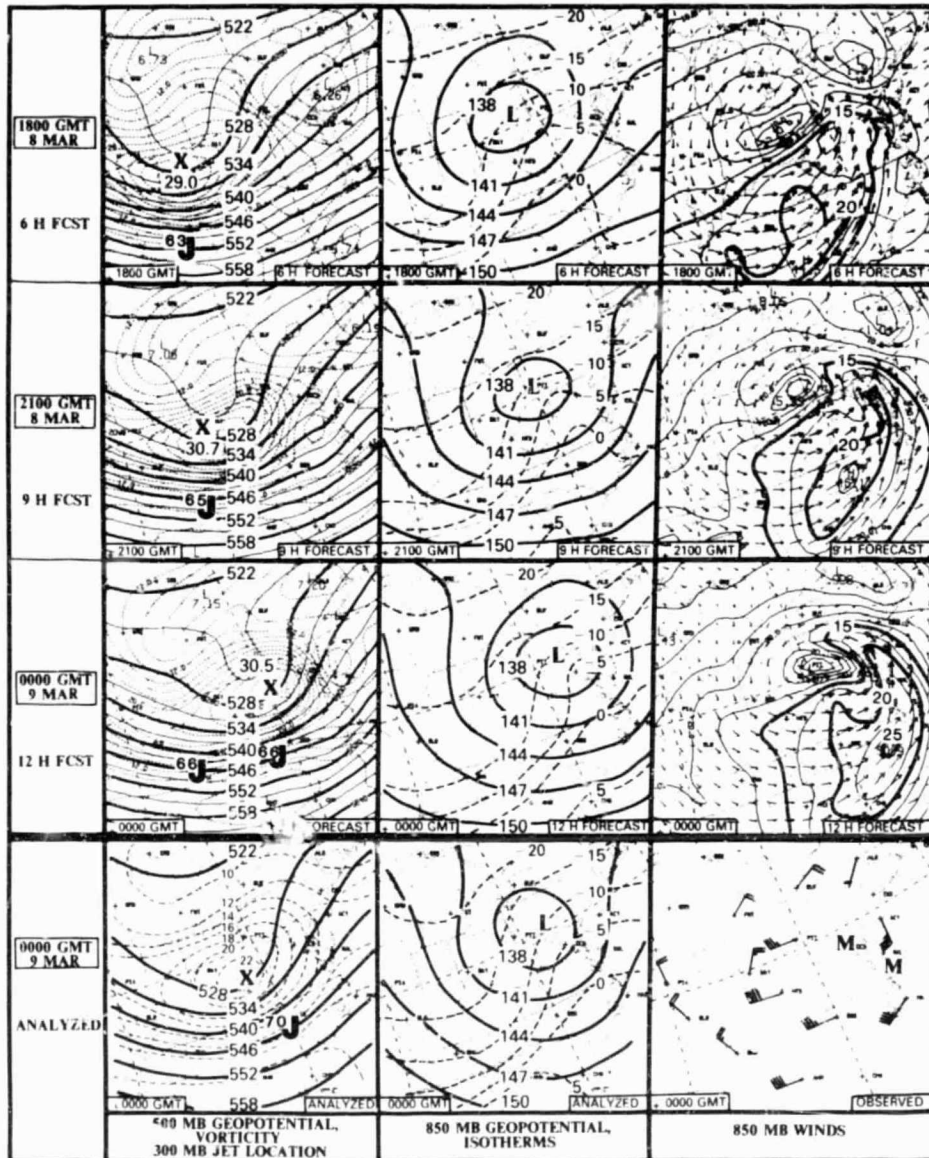


Figure 6. Three-hourly MASS forecasts of selected 300 mb, 500 mb, and 850 mb fields between 1800 GMT 8 March and 0000 GMT 9 March 1984 from model initialized at 1200 GMT 8 March 1984. Verifying analyses at 0000 GMT 9 March are located at the bottom of the figure. The left-hand column includes 500 mb heights (solid, 540 = 5400 m), absolute vorticity (thin dashed; x's denote vorticity maxima; 29.7 = $29.7 \times 10^{-5} \text{ s}^{-1}$), and locations of 300 mb jet maxima (denoted by a J; 65 = 65 m s^{-1}). Vorticity analysis at 0000 GMT 9 March taken from LFM analysis. The middle column includes 850 mb heights (solid, 138 = 1380 m) and isotherms (dashed, $^{\circ}\text{C}$). The right-hand column (forecasts only) includes 850 mb wind vectors and isotachs (solid, m s^{-1}). Observed winds (bottom right) feature wind barbs (each barb represents 5 m s^{-1} ; each half barb represents 2.5 m s^{-1} ; M denotes missing observations).

to 100 km too far to the east. The model accurately predicts the location of the absolute vorticity maximum over West Virginia, but its magnitude ($30 \times 10^{-5} \text{ s}^{-1}$) is larger than diagnosed ($23 \times 10^{-5} \text{ s}^{-1}$), a probable reflection of different grid increments employed. The forecast of the location of the 300 mb jet maximum and its associated wind speeds (not shown) are consistent with observations, but missing wind reports near the core of the jet over the Carolinas at 0000 GMT 9 March make a strict comparison difficult.

At lower levels, MASS correctly predicts the location and depth of the 850 mb low center across Pennsylvania at 0000 GMT 9 March. The 850 mb temperatures are also predicted relatively well with the forecast 0°C isotherm located near its analyzed location along the Virginia-North Carolina border. The 850 mb forecast temperatures are remarkably accurate for many of the reporting rawinsonde stations across the northeastern United States, with no more than a 1°C error (a slight warm bias) at most sites. The only serious flaw is seen near Dayton, OH where the forecast temperature is 5°C warmer than observed, as MASS underestimated the strength of the cold advection to the rear of the 850 mb low center. Verification of the MASS 850 mb wind forecast at 0000 GMT is plagued by missing wind reports at IAD and Wallops Island, VA. However, the MASS forecast of strong west-to-southwesterly flow over North Carolina and southerly flow near Atlantic City, NJ appears to be consistent with observations in those areas. The only significant error is found at Pittsburgh, PA, where the forecast wind speed is 13 m s^{-1} lower than observed.

A closer examination of the MASS forecasts of 500 mb geopotential and vorticity, 300 mb wind speed maxima, and 850 mb geopotential, winds and temperatures verifying at 1800 GMT, 2100 GMT and 0000 GMT provides some clues for processes responsible for the outbreak of convection between 2100 and 0000 GMT. The model simulations show the propagation of an intense 500 mb vorticity maximum from southern Indiana to West Virginia in the 6 h period ending at 0000 GMT 9 March. A region of strong positive vorticity advection is located across West Virginia, Virginia and Maryland at 2100 GMT and 0000 GMT as the vorticity gradient increases in magnitude. The 300 mb wind forecast shows the propagation of a 65 m s^{-1} jet maximum from southern and eastern Tennessee at 1800 GMT and 2100 GMT to North Carolina by 0000 GMT. Therefore, the convective outbreak appears to develop in the diffluent left exit region of the upper-level jet streak, a preferred region of upper-level divergence and mid-tropospheric ascent.

The 850 mb MASS forecast shows the rapid development of a 20 m s^{-1} southerly low-level jet streak across the Washington, DC area at 2100 GMT that moves to the east in the ensuing 3 h period. Note that the forecast jet is associated with a highly confluent (and also convergent) wind field. The coherent structure of upper- and lower-level jet streaks and the development of the low-level jet streak beneath the exit region of the upper-level jet suggests that the model may be simulating the "coupling" process between upper- and lower-level jets, as discussed by Uccellini and Johnson (1979). This process, in combination with boundary layer heating, could act to establish an environment conducive to intense convection through differential moisture and temperature advections. A more detailed diagnostic study of the model output would be necessary to resolve the

mechanisms that influenced the precursor conditions for the convection, and are beyond the scope of this study. However, the model demonstrates that the dynamical processes associated with the jet streaks operated within a 6 h period, indicating that the 12-hourly operational radiosonde network would not be sufficient to properly resolve such occurrences.

d. Model Forecast of 700 mb Vertical Motions, Lifted Index, and Precipitation Amounts

A major aspect of the case that was largely unpredicted and especially difficult to infer from larger-scale models (Fig. 4) was the intense burst of snowfall in the Washington-Baltimore metropolitan areas between 2100 GMT 8 March and 0000 GMT 9 March 1984. MASS provides several diagnostic fields that could have aided in forecasting this event, such as the forecasts of 700 mb vertical motion, the lifted index, and the amount of stable and convective precipitation (Fig. 7).

At 1500 GMT, MASS predicts a comma-shaped pattern of ascent across Ohio and West Virginia with a $-12.7 \mu b s^{-1}$ maximum across southeastern Ohio, where moderate to heavy snows were reported. A lifted index minimum is forecast to decrease from an analyzed value of 4 over central Kentucky at 1200 GMT (not shown) to a value of 2 over western West Virginia at 1500 GMT, indicating a moderate risk for convection. The stable precipitation forecast valid at 1500 GMT indicates generally light 3 h accumulated precipitation amounts (less than 0.25 cm) across Ohio and surrounding states (which was slightly less than observed) with no convective precipitation amounts predicted.

ORIGINAL PAGE IS
OF POOR QUALITY

MASS (3.0) 3-HOURLY FORECASTS OF
700 MB VERTICAL MOTION, LIFTED INDEX
AND PRECIPITATION

MODEL INITIALIZED AT 1200 GMT 8 MARCH 1984

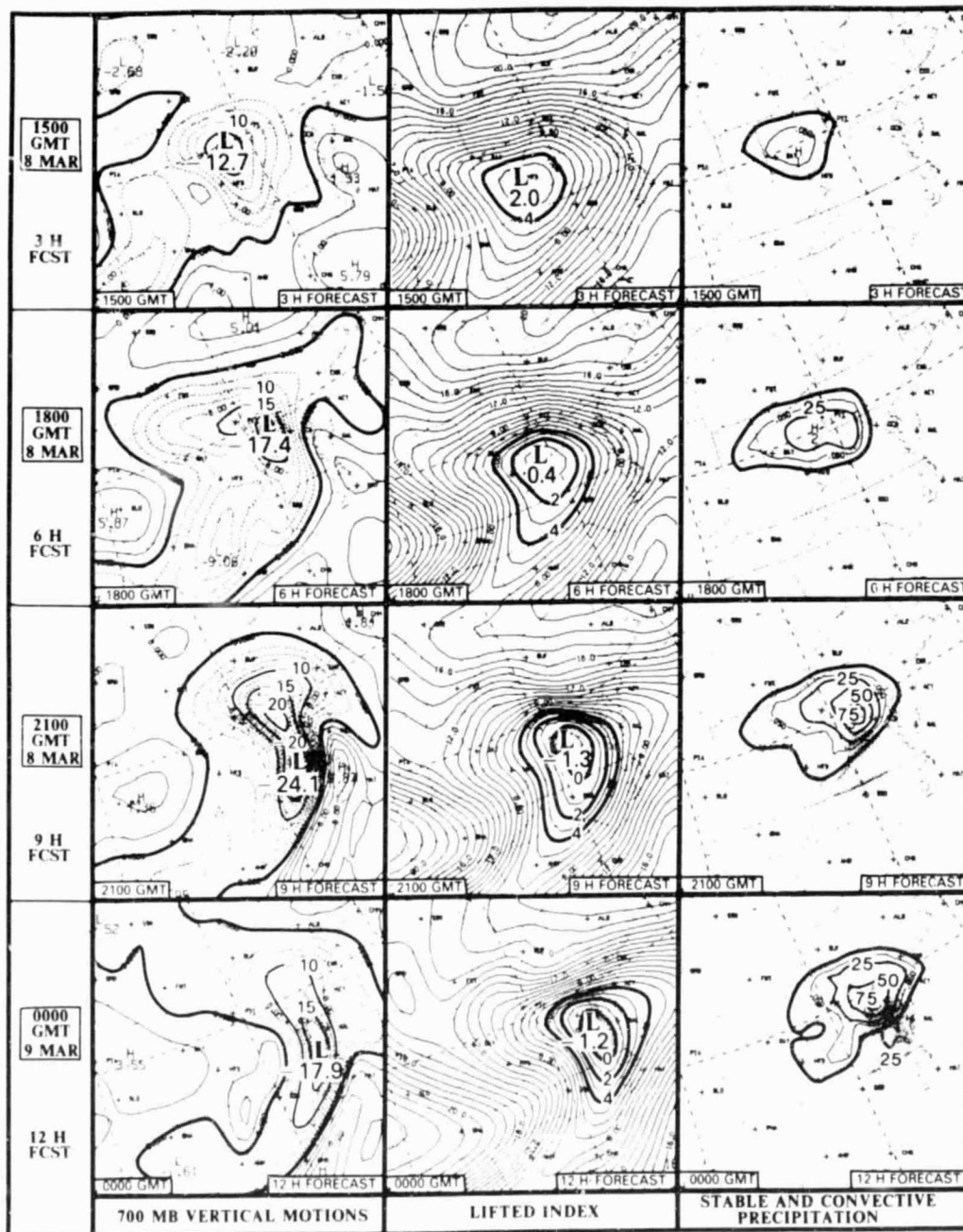


Figure 7. Three-hourly MASS forecasts of 700 mb vertical motion ($-12.7 = -12.7 \mu b s^{-1}$; thick solid line separates ascent and descent), lifted index (thick solid lines are in increments of 2 for values less than 4; shading is for values less than 0), and three-hourly accumulated stable (solid contours) and convective (shaded regions) precipitation ($25 = 0.25 \text{ cm}$) between 1500 GMT 8 March and 0000 GMT 9 March 1984 from model initialized at 1200 GMT 8 March 1984.

By 1800 GMT, the vertical motion forecast continues to show a comma-shaped pattern of ascent with the predicted center concentrated over northeastern West Virginia, where it amplifies to $-17.4 \mu\text{b s}^{-1}$. This forecast center is located just to the northeast of the newly developing cloud band over West Virginia, as depicted by the infrared satellite imagery (Fig. 3). The lifted index minimum is predicted to advance to central West Virginia and has dropped to a value near zero. The stable precipitation forecast shows increasing precipitation amounts (now in excess of 0.25 cm in 3 h) over eastern Ohio, northern West Virginia and southwestern Pennsylvania. Surface observations at 1800 GMT (Fig. 5) indicated a band of moderate to heavy snow from extreme northeastern Indiana, north-central Ohio into southeastern Ohio, southwestern Pennsylvania and northern West Virginia. No convective precipitation is forecast as yet by the model.

By 2100 GMT, the vertical motion forecast now simulates two centers of increasing ascent, one at $-19 \mu\text{b s}^{-1}$ over western Maryland and the other at $-24 \mu\text{b s}^{-1}$ across south-central Virginia. The two centers are imbedded in a line of maximum ascent that is colocated with the observed line of convection visible on the infrared imagery from South Carolina to central Virginia (Fig. 3), as well as with the surface observations of developing thunderstorms in the same area. The model continues to forecast a decrease in the lifted index to -1.3 over northern Virginia. The increasing ascent and decreasing potential stability are occurring near the axis of the low-level jet beneath the exit region of the upper-level jet (Fig. 6) in a preferred region for ascent (Beebe and Bates, 1955). The 3 h quantitative stable precipitation forecast shows that precipitation rates have increased

substantially since 1800 GMT with a maximum of greater than 0.75 cm just to the west of Washington, DC over the panhandles of Maryland and West Virginia. The model's convective precipitation forecast now indicates measureable, but still light, amounts across central Virginia and north-central North Carolina, which were observed at this time.

At 0000 GMT 9 March, the model simulation of the 700 mb vertical motion shows a consolidated ascent maximum from eastern Pennsylvania through eastern Virginia southward into South Carolina with a maximum of $-17.9 \mu\text{b s}^{-1}$ across southeastern Virginia, where moderate to heavy thunderstorms were occurring. The MASS forecast of ascent at 0000 GMT also differs considerably from the corresponding LFM forecast (Fig. 4). MASS generates a more distinct narrow, elongated pattern, as well as producing magnitudes four times greater than those predicted by the LFM. The forecast lifted index values have leveled off and remain between -1 and -2 at 0000 GMT with the center located across eastern Virginia. The stable precipitation forecast shows a maximum rate of 0.75 cm in 3 h between Washington, DC and Baltimore, MD, with a sharp gradient of precipitation amounts located across Maryland and northern Virginia. This distribution compares favorably with a local observing network that measured heaviest precipitation amounts primarily to the north of Washington. At DCA and points further south and east, observed melted precipitation amounts of 0.75 cm or less fell generally during the storm, while amounts ranging between 1.0 and 1.5 cm fell elsewhere, consistent with the model forecast. The 3 h convective forecast indicates a maximum 3 h amount of 0.25 cm over eastern Virginia, but actual reports indicate somewhat larger amounts in localized areas.

e. Model Forecast of the Rain-Snow Line

Two indicators that are frequently used to determine the location of the rain-snow line are the 1000 to 500 mb thickness (Lamb, 1955; typical values are 5400 to 5430 m in the Middle Atlantic states during the winter season), and the 850 mb 0°C contour. In this case, the analyzed 5400 m thickness contour remained across southern Virginia (not shown) while the 0°C isotherm at the 850 mb level had barely progressed northward to the North Carolina-Virginia border by 0000 GMT 9 March (Fig. 6).

MASS forecast the 5400 m thickness contour (not shown) and the 850 mb 0°C isotherm to move no further north than southern Virginia. Thus, both the observed and model-predicted thickness and 850 mb temperatures indicated that the precipitation north of the North Carolina-Virginia border would fall as snow. Yet, rain showers fell as far north as Washington, DC and points south and east as surface temperatures approached 5°C at 2100 GMT (Figs. 2, 5), while the northern and western suburbs of Washington recorded heavy snowfall with surface temperatures at 0°C or lower. It appears that warm advection in the lowest 50 mb of the atmosphere and late-winter solar heating to the south and east of the developing secondary low center were sufficient to cause snow to change to rain before reaching the ground. The MASS predictions of air temperature in the lowest model layer (equivalent to a 60 mb layer centered at 964 mb) provided a possible indicator of the location of the rain-snow line, as shown in Fig. 5. At 1500 GMT, MASS forecast the 0°C isotherm in the lowest model layer to lie south of Washington, DC. The 0°C isotherm was forecast to move northward in the following 3 to 6 h to a region between Washington and Baltimore. Observations at 2100 GMT show that the forecast field is an

excellent predictor of surface air temperatures as observed values of -1°C at Baltimore, 4°C at Washington-National, and nearly 10°C at Richmond, VA are very close to the forecast values. Thus, forecasters could have benefited from this information to help resolve the evolution of the rain-snow line in a situation where rain would not have been predicted as far north as Washington, DC from thickness and 850 mb considerations. The 0000 GMT temperature forecast failed to capture the sudden drop of temperature across northern Virginia and central Maryland, but did capture the strong cold advection across western Virginia and West Virginia at this time.

f. Summary of the 8 March 1984 MASS Simulation

The MASS simulation of the 8 March 1984 thunder/snow burst in the Washington-Baltimore metropolitan area demonstrates that the model provides mesoscale information that potentially could have had a significant positive impact on local forecasts for this case. The model predicted decreasing values of the lifted index, indicating an increasing potential for convection across Virginia and Maryland by 2100 GMT, and then predicted convective precipitation to develop between 2100 and 0000 GMT. In addition, a correct forecast of the timing and location of secondary surface cyclogenesis coincided with the outbreak of convection, while the forecast vertical motions and stable precipitation amounts corresponded well with satellite imagery and surface observations. Finally, the model prediction of temperatures in the lowest model layer provided a remarkably accurate depiction of the rain-snow line.

4. THE 28 MARCH 1984 NORTH AND SOUTH CAROLINA TORNADO OUTBREAK

a. Surface and Weather Analyses

The 28 March 1984 cyclone/severe weather case will long be remembered along the East Coast of the United States as one of the most destructive in many years. A series of tornadoes across South and North Carolina was responsible for the most lethal severe weather outbreak in the United States in ten years with 57 deaths and 1,248 injuries.¹ The tornadoes developed within the circulation of an exceptionally large and deep mid-latitude cyclone that set numerous low barometric records across the Tennessee Valley, the Southern and Middle Atlantic states.² The cyclone was associated with many other forms of severe weather, including wind-driven tidal surges that caused widespread damage from the Middle Atlantic to New England coasts, and an early spring snowstorm across the Northeast that produced up to 75 cm of snow across interior sections of Pennsylvania, New York, and New England. While the storm presented a challenging array of meteorological phenomena from a forecasting perspective, the severe weather outbreak across the Carolinas was forecast extremely well by National Weather Service personnel.

The tracks and times of occurrence of the 22 reported tornadoes across South and North Carolina are shown in Fig. 8. The tornado outbreak was

¹March 1984 Storm Data statistics.

²The cyclone that spawned the severe weather outbreak developed on 27 March over Texas, where temperatures ranged from near 0°C with snow falling across the panhandle to near 40°C over the extreme south. Superheated Mexican air set several temperature records, including the 41°C maximum at Brownsville, TX, which was the highest temperature ever recorded at that station.

ORIGINAL PAGE 5
OF POOR QUALITY

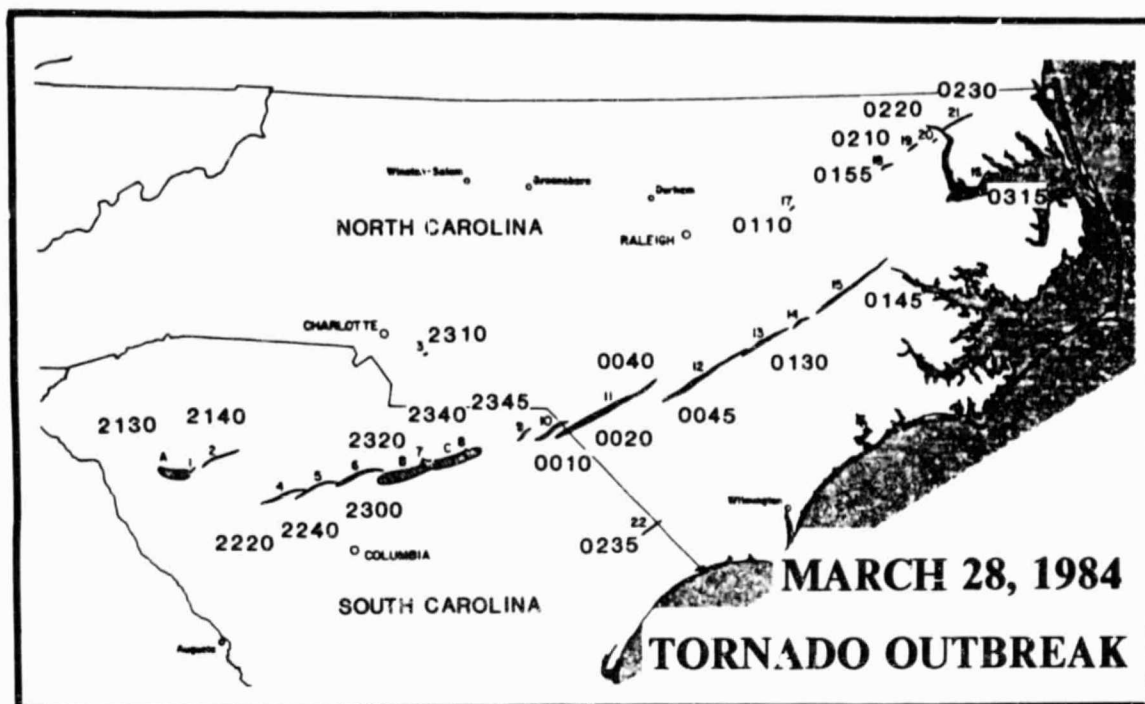


Figure 8. Tornado paths and times of occurrences (GMT) (from March 1984 Storm Data) between 2100 GMT 28 March 1984 and 0300 GMT 29 March 1984.

spread over a 6 h period beginning after 2100 GMT 28 March across northwestern South Carolina and ending in extreme northeastern North Carolina shortly after 0300 GMT 29 March. Scattered tornadoes were also reported earlier across Alabama and Georgia. Many of the most intense tornadic storms formed along a nearly straight line that extended from north-central South Carolina to eastern North Carolina, lasting over 5 h. The paths of the individual storms ranged from 73 to 500 km with a maximum width of 4 km.

A six-hourly sequence of surface weather maps between 1800 GMT 28 March and 0600 GMT 29 March is presented in Fig. 9 to highlight the synoptic conditions prior to and during the tornado outbreak. At 1800 GMT, a large, intensifying cyclone consisted of multiple centers, including a 984 mb low over west-central Tennessee, a 982 mb low over eastern Kentucky, a 988 mb center across north-central North Carolina, and a recently formed 985 mb center over eastern Alabama and western Georgia, where three-hourly pressure falls exceeded -6 mb (3 h)^{-1} . Warm, humid air covered the southeastern United States with temperatures exceeding 25°C and dewpoint temperatures approaching 20°C as far north as North Carolina. Rains were widespread across the eastern half of the United States and were mixing with or changing to snow across parts of Pennsylvania and New York, where surface temperatures were falling toward 0°C as the damming of cold air east of the Appalachians became a dominant feature.

Between 1800 GMT 28 March and 0000 GMT 29 March, thunderstorms grew rapidly across Georgia and the Carolinas with numerous tornadoes reported in Georgia, South Carolina, and North Carolina. The Alabama-Georgia low moved rapidly east-northeastward along a nearly stationary front that

ORIGINAL PAGE IS
OF POOR QUALITY

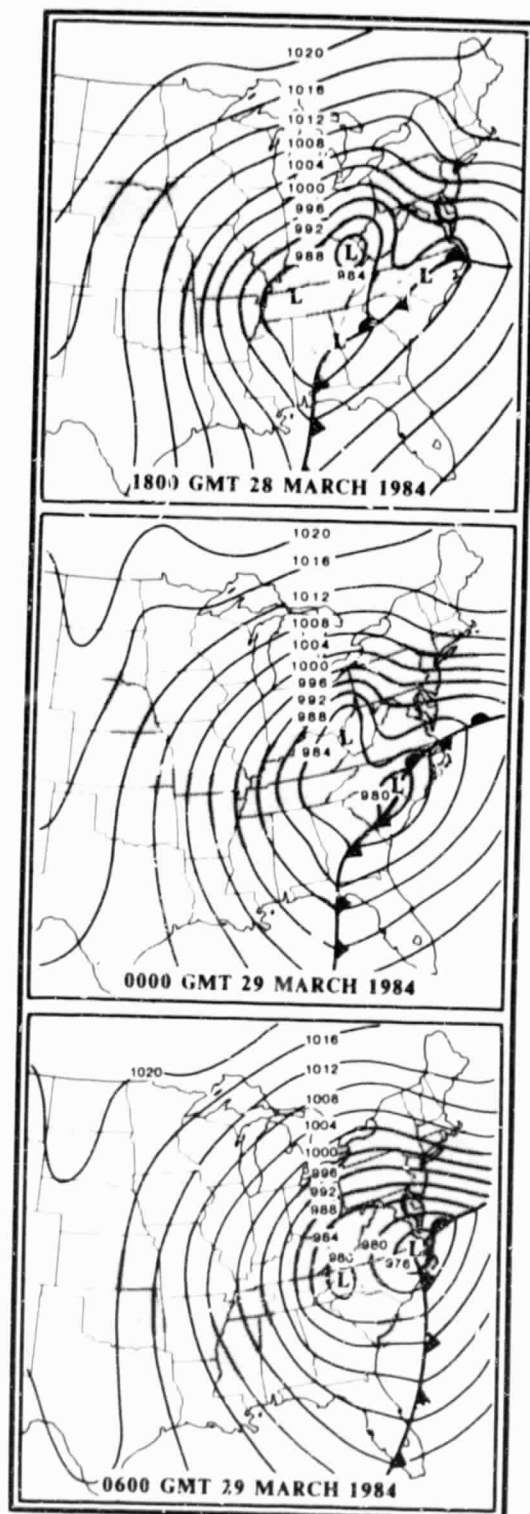


Figure 9. Sea-level pressure (mb) and surface frontal analyses for 1800 GMT 28 March, 0000 GMT 29 March, and 0600 GMT 29 March 1984. Shading represents precipitation occurring at the time of the analysis.

extended from Georgia to the North Carolina-Virginia border. The low deepened from 985 mb at 1800 GMT to 977 mb near Athens, GA by 2100 GMT, a fall of 8 mb in only 3 h. In the following 3 h, the low moved across western South Carolina and by 0000 GMT was located over the North-South Carolina border, maintaining a central pressure of approximately 977 mb. In the warm sector ahead of this rapidly evolving low center, winds backed to a south-southeasterly direction prior to the onset of thunderstorms and increased markedly in speed.

The low center began to deepen again after 0300 GMT, following a 6 h period of little or no intensification, reaching 974 mb near Norfolk, VA by 0600 GMT. Tornadoes crossed eastern North Carolina before dissipating around 0300 GMT. By 0600 GMT, intense thunderstorms were confined to extreme northeastern North Carolina and southeastern Virginia. The severe weather did not progress further north than extreme southeastern Virginia where colder air remained entrenched at the surface. Snow was falling across southern New York, northern New Jersey, Pennsylvania, and parts of Maryland. Following 0600 GMT, winds along the Middle Atlantic and New England coasts increased out of a northeasterly direction as the low tracked northward through eastern Virginia, Maryland, and Delaware, deepening to 966 mb along the Middle Atlantic coast by 1200 GMT 29 March. The high wind speeds and long easterly fetch contributed to severe beach erosion along the shoreline.

A sequence of infrared satellite images at 1800 GMT, 2100 GMT, and 2300 GMT 28 March and 0100 GMT and 0330 GMT 29 March presented in Fig. 10 shows the widespread region of clouds across the eastern United States that produced moderate to heavy precipitation late on 28 March. The satellite



Figure 10. Selected SMS-GOES infrared satellite imagery between 1800 GMT 28 March and 0330 GMT 29 March 1984, which covers the period of the Carolinas tornado outbreak. Figure includes surface low positions and c refers to the expanding region of colder cloud top temperatures.

images depict the development of a mesoscale convective system (MCS) over central Alabama and northern Georgia by 1800 GMT. The MCS expanded rapidly in size as it moved to northeastern Georgia and northwestern South Carolina by 2100 GMT, as the tornado outbreak began. Between 2300 and 0100 GMT, with the tornado outbreak in progress across South and North Carolina (refer to Fig. 8), the area of colder cloud tops associated with the convection expanded in areal extent, covering South Carolina, North Carolina, and Virginia. By 0330 GMT, the MCS covered eastern North Carolina and much of the Middle Atlantic states as the tornado outbreak had ended (at least over land). The area of convection in this region continued to expand in areal coverage during the following 12 h in conjunction with the developing cyclone along the East Coast and became a large comma-shaped cloud mass over the eastern United States by the morning of 29 March.

b. Model Forecast of Sea-Level Pressure and Pressure Tendency

The MASS forecast initialized at 1200 GMT 28 March 1984 is examined from 1800 GMT 28 March through 0300 GMT 29 March, the period when severe convection was occurring across the southeastern United States. Sea-level pressure and pressure tendency forecasts for 1800 GMT and 2100 GMT 28 March, and 0000 GMT and 0300 GMT 29 March are compared against corresponding observed surface analyses in Fig. 11. The forecast of sea-level pressure verifying at 1800 GMT 28 March has a 985 mb low center in northeastern Tennessee with a low pressure trough extending southward into central Alabama and another trough extending eastward along the North Carolina-Virginia border. The verifying surface analysis indicates that a

3-HOURLY SURFACE ANALYSES AND
MASS (3.0) FORECASTS
MODEL INITIALIZED AT 1200 GMT 28 MARCH 1984

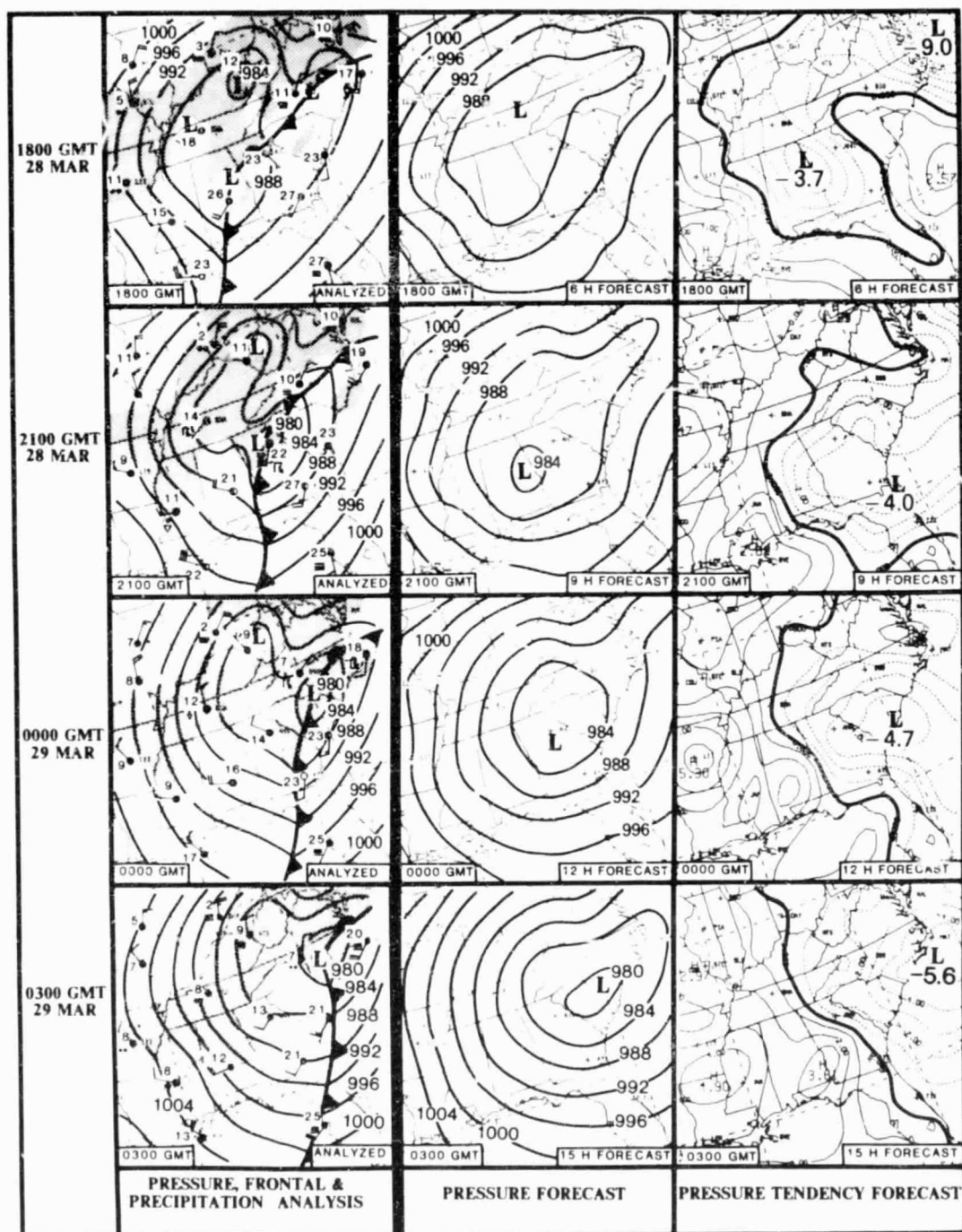


Figure 11. Three-hourly surface analyses and MASS forecasts between 1800 GMT 28 March and 0300 GMT 29 March 1984 from model initialized at 1200 GMT 28 March 1984. See Figure 5 for additional details. Note that isotherm analysis and forecast is not included here.

985 mb low center had already formed in eastern Alabama by this time, indicating that the model was not fully resolving the initial development of the low pressure system that was to become the dominant cyclone. Furthermore, the model overdeepens the trough that extends eastward to the Virginia-North Carolina border by nearly 4 mb. The $-9.0 \text{ mb (3 h)}^{-1}$ pressure fall forecast off the Virginia coast between 1500 and 1800 GMT (Fig. 11) is an indication that the model was overdeveloping this part of the system, as well as a rapidly intensifying region of stable precipitation (not shown).

In the following 3 h, MASS develops a distinct 984 mb low center over eastern Alabama, approximately 250 km west of the observed surface low in northern Georgia (Fig. 11). The model prediction of 2 to 3 mb pressure falls in eastern Alabama and Georgia between 1800 and 2100 GMT (Fig. 11) is far less than the 10 mb local falls observed across northern Georgia, as the central pressure of the low deepened 8 mb in 3 h to 977 mb near Athens, GA. It also appears that the northward movement and deepening of the trough extending along the Virginia-North Carolina border have ceased in the MASS forecast by 2100 GMT (Fig. 11). The position of this feature is in reasonably good agreement with observations.

The 0000 GMT and 0300 GMT simulations of the low center tracking across eastern Georgia (0000 GMT) and northeastern South Carolina (0300 GMT) continue to lag the observed locations by approximately 200 km and by 3 to 4 h. The model deepens the low at a rate of -1 mb h^{-1} between 2100 GMT and 0300 GMT, although the observed center did not appear to deepen at all during this period. However, since the forecasts failed to

capture the rapid deepening between 1800 and 2100 GMT, the predicted 978 mb central pressure by 0300 GMT is within 1 mb of the actual pressure.

While the MASS forecasts failed to accurately simulate the rapid deepening and movement of the low center across the southeastern United States, it fared no worse than the LFM forecast initialized at the same time. A comparison of the MASS and LFM 12 h forecast sea-level pressure fields at 0000 GMT 29 March with the observed pressure analysis (Fig. 12) indicates that both models erroneously predicted the position of the low. The LFM forecast places a 981 mb low center over northeastern Tennessee, while MASS forecasts a 981 mb center over eastern Georgia. In reality, the 977 mb low center was located near the South-North Carolina border. Although both models were substantially in error, the actual track of the low across Alabama, Georgia, and the Carolina was forecast well by the 3 h MASS output, although the MASS prediction lagged the actual center position by 3 h.

c. Model Forecast of Upper-Level Fields

MASS forecasts of 500 mb geopotential and vorticity, locations of 300 mb wind speed maxima, and 850 mb geopotential, winds, and temperatures at 1800 GMT 28 March through 0300 GMT 29 March are shown in Fig. 13. The MASS 12 h forecasts verifying at 0000 GMT 29 March are benchmarked against analyses derived from 0000 GMT rawinsonde observations.

At 300 mb, MASS predicts an intense upper-level jet streak over the southeastern United States with a 75 m s^{-1} 300 mb speed maximum over southeastern Alabama at 0000 GMT. The diffluent exit region of this jet is forecast over Georgia, South Carolina, and North Carolina. The predicted

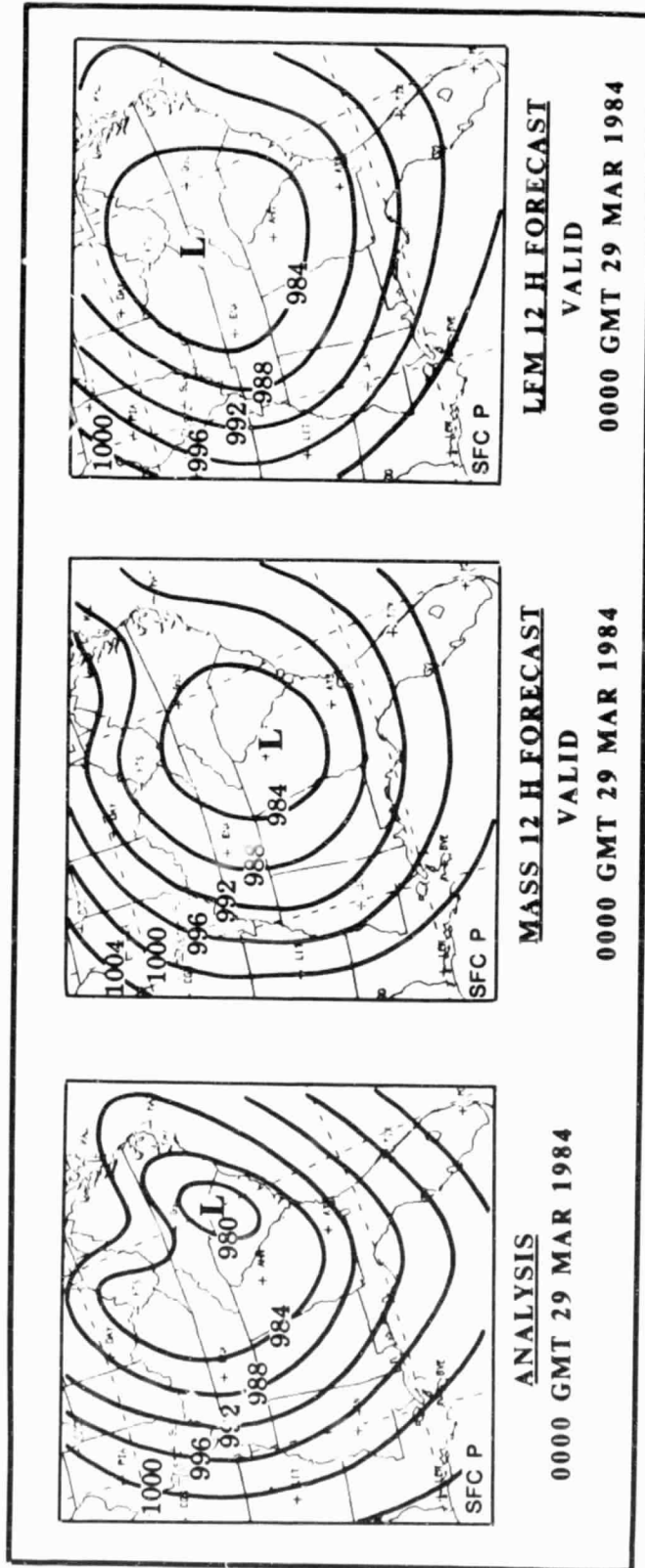


Figure 12. Analysis and 12 h MASS and LFM forecasts of sea-level pressure at 0000 GMT 29 March 1984.

MASS (3.0) 3-HOURLY FORECASTS OF
SELECTED 300 MB, 500 MB and 850 MB
FIELDS

MODEL INITIALIZED AT 1200 GMT 28 MARCH 1984
VERIFYING ANALYSES AT 0000 GMT 29 MARCH 1984

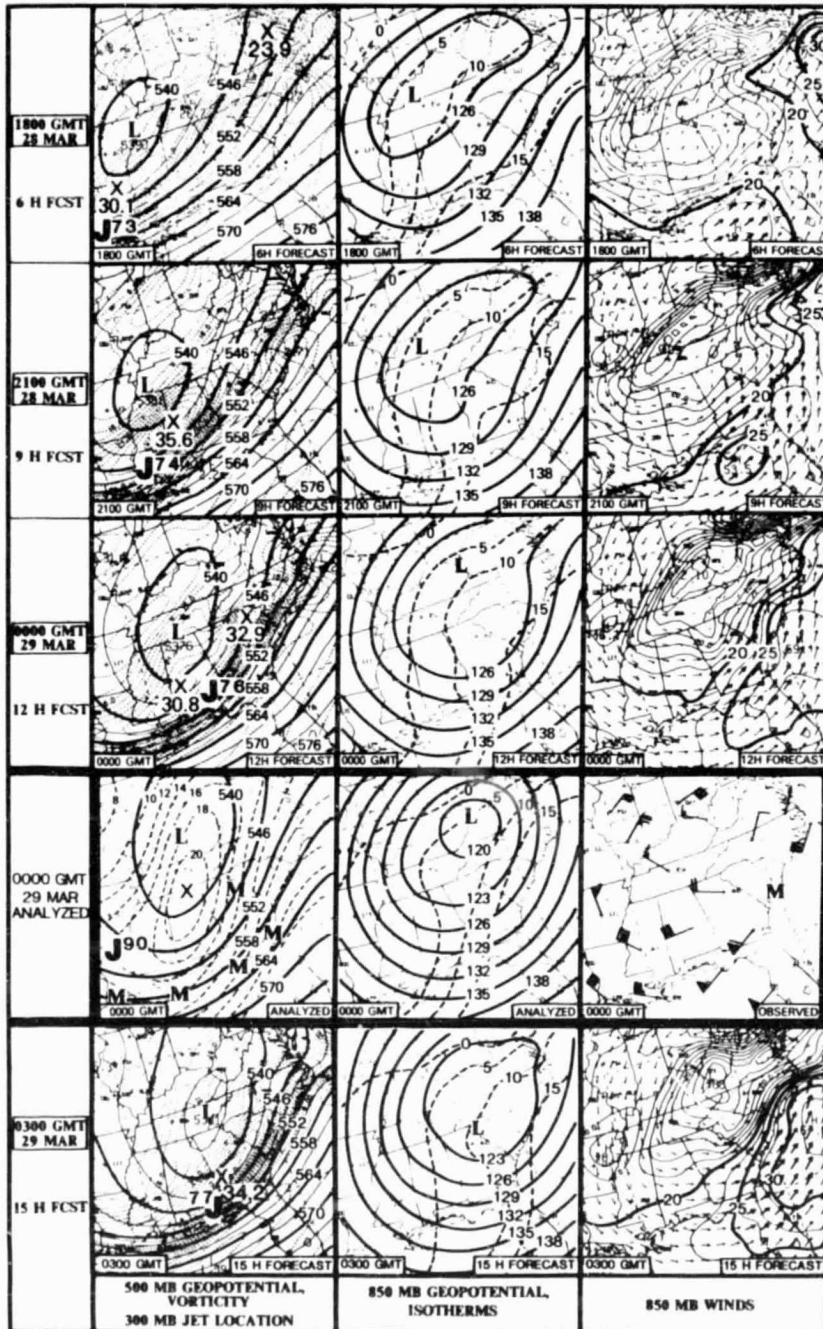


Figure 13. Three-hourly MASS forecasts of selected 300 mb, 500 mb, and 850 mb fields between 1800 GMT 28 March and 0300 GMT 29 March 1984 from model initialized at 1200 GMT 28 March 1984. The verifying analyses at 0000 GMT 29 March 1984 appear immediately below the 0000 GMT forecasts. See Figure 6 for additional details.

location of the 300 mb wind maximum at 0000 GMT is well to the east of a 90 m s^{-1} jet maximum analyzed over northern Louisiana. However, many wind reports at 300 mb were missing across the southeastern states at 0000 GMT 29 March (see the analysis above the bottom left panel in Fig. 13), which make detailed comparisons between model forecast and observations very difficult for this case.

At 500 mb, the forecast captures the orientation of the deep upper-level trough at 0000 GMT 29 March, but displaces the center of lowest geopotential heights and maximum absolute vorticity approximately 300 km to the south of their observed locations. The sequence of vorticity maps from 1800 GMT to 0300 GMT in Fig. 13 indicates that a succession of vorticity maxima generated by the model propagates along the direction of the 500 mb flow. This type of detail cannot be confirmed using the operational data base. However, several vorticity features can be followed and discussed with respect to other forecast fields. One vorticity maximum develops near the North Carolina-Virginia border shortly after the model is initialized at 1200 GMT 28 March, propagates northeastward, and is located in Virginia by 1800 GMT (Fig. 13). The positive vorticity advection associated with this maximum is concentrated along the Middle Atlantic coast during the same period when a large region of stable precipitation is overforecast and the surface trough is overdeepened by the model (Fig. 11). It thus appears that this vorticity feature might be a spurious development by the model, which may be an artifact of an improper specification of the vertical distribution of latent heating through the cumulus parameterization scheme (e.g., see Anthes and Keyser, 1979). A second vorticity maximum is located near the base of the 500 mb trough over northern Louisiana at 1800 GMT

(Fig. 13). This maximum appears to propagate and extend itself toward the east-northeast so that the maximum positive vorticity advection is located over South Carolina and North Carolina at 0000 GMT and 0300 GMT, the times when tornadoes were occurring in these states.

The 850 mb forecasts (Fig. 13) show several low-level jet streaks for this case, one off the Carolina coast and the other in the Gulf of Mexico at 1800 GMT. The 30 m s^{-1} low-level jet streak off the Carolina coast is associated with the overdeveloped precipitation and surface trough discussed earlier. The 22 m s^{-1} low-level jet in the Gulf of Mexico amplifies rapidly to nearly 35 m s^{-1} as it moves to near the Carolina coast by 0300 GMT. As the low-level jet propagates northeastward, winds in South Carolina back to a more southerly direction and increase to greater than 25 m s^{-1} along the coast. The 850 mb wind forecast valid at 0000 GMT appears to be fairly representative of observed winds across the Southeast, especially at Waycross, GA and Cape Hatteras, NC, although actual speeds were slightly higher. The jet maximum off Charleston, SC is difficult to verify since Charleston's winds were missing. The 850 mb geopotential forecast reflects the observed location of the 850 mb low center, although the geopotential values are 30 to 40 m higher than analyzed. The 850 mb temperature forecast captures the strong temperature gradient across Virginia, but the observed warming across the Southeast valid at 0000 GMT is forecast weakly by the model, with the predicted temperature at Cape Hatteras, NC, 4°C lower than in reality. Nevertheless, the model is predicting significant warm air advection in the Carolinas by 0000 GMT in conjunction with the increasing 850 mb south to southwesterly low-level jet. There again is the possibility that the model is simulating the

coupling of the low-level jet in the exit region of the upper-level jet streak immediately prior to the outbreak of convection in the South and North Carolina region.

d. Model Forecast of 700 mb Vertical Motions, Lifted Index, and Precipitation Amounts

Three-hourly model simulations of 700 mb vertical motions, lifted index and convective precipitation (Fig. 14) are examined to determine if MASS provided an indication of the convective potential across the southeastern United States between 1800 GMT 28 March and 0300 GMT 29 March 1984, despite the deficiencies in the sea-level pressure forecast emphasized earlier. The vertical motion forecasts indicate an ascent maximum of $-11 \mu\text{b s}^{-1}$ across Alabama at 1800 GMT that splits into several centers. One center amplifies across Georgia and the Carolinas between 2100 GMT and 0000 GMT to a maximum value of $-16 \mu\text{b s}^{-1}$ over the western South Carolina-North Carolina border. In the 3 h period ending at 0300 GMT, the ascent maximum roughly doubles to $-32 \mu\text{b s}^{-1}$ just to the east of Cape Hatteras, NC. Therefore, the model predicts a threefold increase in the magnitude of ascent across South and North Carolina between 2100 GMT and 0300 GMT that coincides with the period in which the explosive growth of convection and the outbreak of tornadoes occurred. MASS appears to provide a much better indicator of vertical motions across the Carolinas at 0000 GMT 29 March than the LFM since the 12 h LFM forecast valid at 0000 GMT 29 March indicates that North Carolina lies within a region of minimum ascent of less than $-2 \mu\text{b s}^{-1}$ (not shown).

MASS (3.0) 3-HOURLY FORECASTS OF 700 MB
VERTICAL MOTION, LIFTED INDEX AND
PRECIPITATION

MODEL INITIALIZED AT 1200 GMT 28 MARCH 1984

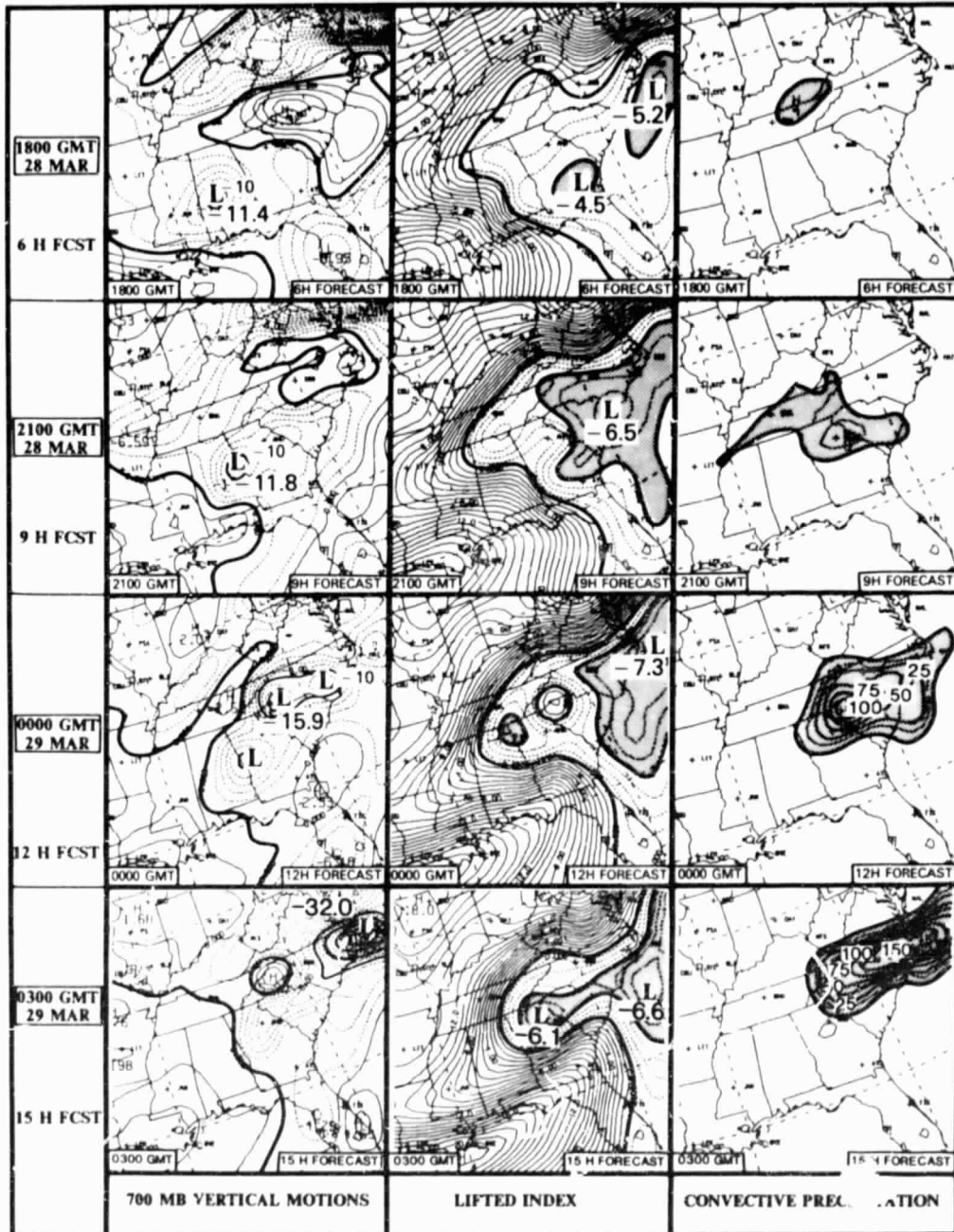


Figure 14. Three-hourly MASS forecasts of 700 mb vertical motion ($-11.4 = -11.4 \mu b s^{-1}$; thick solid lines separate ascent and descent), lifted index (thick solid lines are in increments of 4 for values less than 0; shading is for values less than -4), and three-hourly accumulated convective precipitation ($25 = 0.25$ cm) between 1800 GMT 28 March and 0300 GMT 29 March 1984 from model initialized at 1200 GMT 28 March 1984.

The lifted index prediction provides an indication of the increasing potential for severe weather across the Southeast after 1800 GMT 28 March. The predicted lifted index decreases from minimum values of -4 over southern Georgia at 1800 GMT to -6.5 along the South Carolina coast at 2100 GMT, and to -7.3 near Cape Hatteras, NC by 0000 GMT.

The MASS forecasts for convective precipitation confirm that the increasing potential for convection, as indicated by the decreasing values of lifted index, is being effectively realized by the convective parameterization scheme. A blossoming area of forecast convective rainfall develops across northeastern Georgia and South Carolina at 2100 GMT, covers northern Georgia, South Carolina, and North Carolina at 0000 GMT, and is centered over eastern North Carolina by 0300 GMT. The northern boundary of the predicted convective rainfall advances no further north than southern Virginia as the damming of cold air east of the Appalachians inhibited the northward movement of warm, moist air along the coast. The timing and locations of these simulated features match very closely the regions of convection inferred from the satellite images in Fig. 10. Thus, while the forecast sea-level pressure appears to lag the observations, MASS predicts a major convective outbreak in the Carolinas between 2100 GMT 28 March and 0300 GMT 29 March. The simulation could have aided the forecaster in refining the area and timing of this event.

e. Summary of the 28 March 1984 MASS Simulation

A brief examination of the MASS forecasts initialized at 1200 GMT 28 March indicates that the model could have provided the forecaster several indicators of an increasing risk for convection across the

Carolinas during the late afternoon and early evening of 28 March. These indicators include enhanced ascent, an expanding region of convective precipitation amounts, and decreased potential stability across North and South Carolina between 1800 GMT 28 March and 0300 GMT 29 March. However, the model prediction suffers from the overdevelopment of a sea-level pressure trough in the Middle Atlantic states and a forecast of excessive stable rainfall amounts (not shown). Furthermore, MASS did not capture the rapid deepening and movement of the intense subsynoptic low pressure center across the southeastern United States just prior to the main tornado event. A legitimate question, therefore, remains as to whether the field forecaster might have believed the convective forecast produced by the model after 1800 GMT in light of the spurious development of the Middle Atlantic system prior to 1800 GMT.

It is possible that incorrect specifications of the vertical latent heat distribution and wind fields may have been, in part, responsible for the overdevelopment of precipitation and the sea-level pressure trough in the Middle Atlantic states, as well as the formation of spurious vorticity maxima. Previous studies (Anthes and Keyser, 1979; Anthes et al., 1983; Koch et al., 1984) have noted that numerical models overdevelop regions of precipitation and subsequently enhance sea-level development due to the effects of condensation heating and its vertical distribution. The ability of cumulus parameterization schemes to adequately simulate these processes is currently under study. In addition, the 300 mb analysis at 1200 GMT 28 March (the time of model initialization) indicates that wind reports were missing for seven stations within the intense upper-level jet streak across the southern United States (Fig. 15). The significance of the

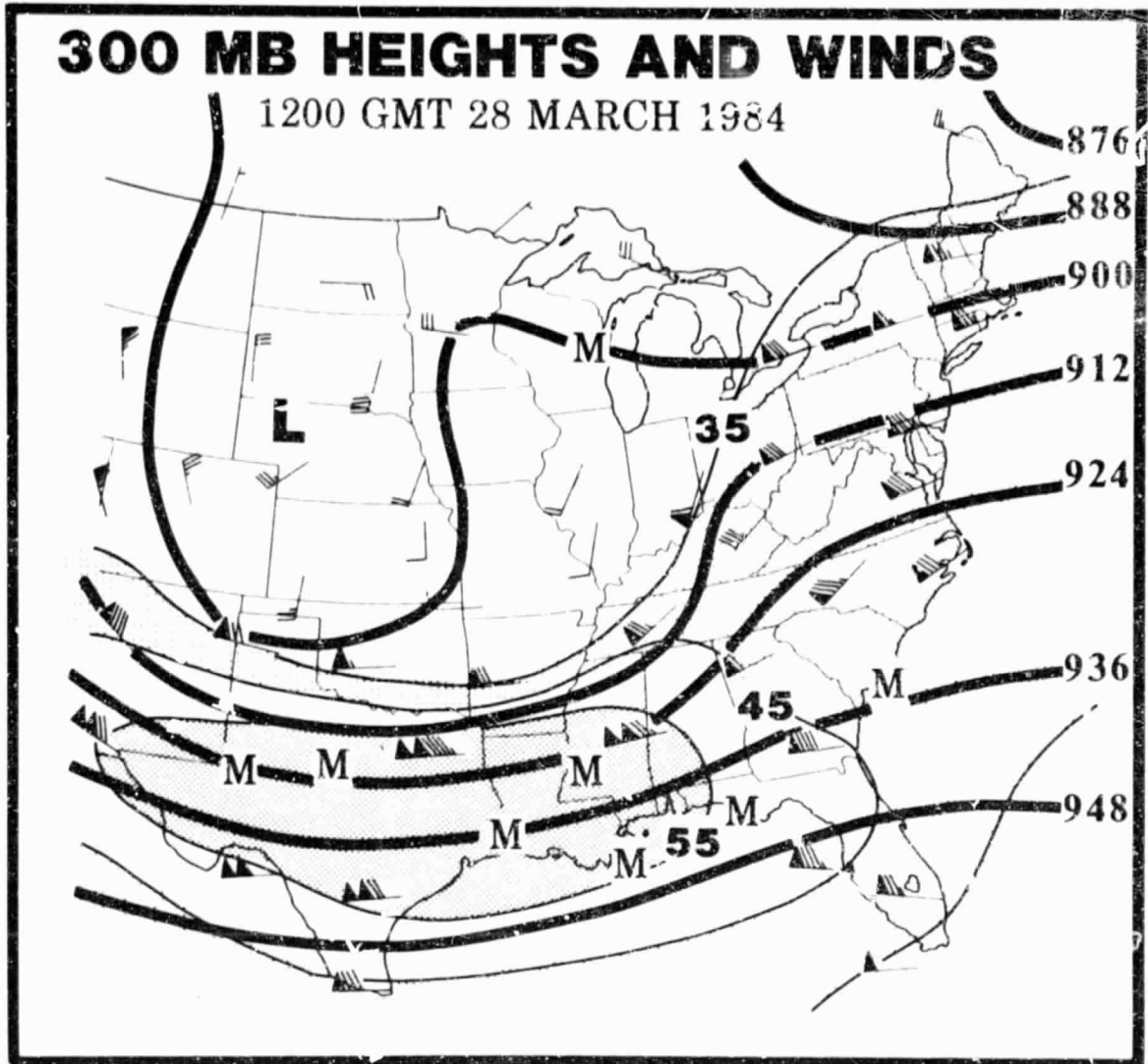


Figure 15. Analysis of 300 mb height (thick solid, 900 = 9000 m) and wind speed (thin solid, m s^{-1}) for 1200 GMT 28 March 1984. Flags represent speeds of 25 m s^{-1} ; barbs represent speeds of 5 m s^{-1} ; half barbs represent 2.5 m s^{-1} speeds. M denotes missing wind reports.

missing wind reports and their effects on prescribing the initial mass and momentum balance within the model cannot be accurately determined.

However, it is likely that an improper representation of the wind speeds associated with the upper-level jet and its subsequent effects on the representation of the initial wind and temperature fields could have contributed to the model deficiencies for this case. Furthermore, the intensity of the overdeveloped trough predicted by the model along the Middle Atlantic coast and its impact on the wind and temperature field along the coast may have helped inhibit the major development further upstream, which was weaker and slower than in reality.

The sensitivities of mesoscale models to wind errors (Chang et al., 1984) and to different specifications of the vertical distribution of latent heating (Anthes et al., 1983) have already been demonstrated. Further, detailed experiments are required to resolve the sensitivity of the 28 March 1984 MASS simulation to different specifications of the upper-level jet and latent heating distributions. It is possible that factors such as these may have a significant bearing on the errors observed in this case.

5. SUMMARY

This paper has described some recent model simulations using the Mesoscale Atmospheric Simulation System (MASS), a mesoscale modeling system that can represent nearly the entire North American continent and can be used in real-time. The model simulations were made for recent East Coast severe weather events, which include a brief but intense outbreak of thunderstorms with snow in the Washington, DC-Baltimore, MD area on 8 March 1984, and the devastating outbreak of tornadoes across South and North Carolina on 28 March 1984. The object of the study was not to prepare a detailed statistical study of model accuracy and biases, as was done by Koch et al. (1984), but rather to illustrate the ability of mesoscale models to simulate dynamical interactions and diabatic processes and possibly provide more useful weather forecasts than are available from current operational models.

The outbreak of heavy snow-producing thunderstorms during the evening rush hour in the Washington, DC-Baltimore area on 8 March 1984 was an event that was poorly predicted by local forecasters and extremely difficult to infer from the larger-scale operational numerical models. Had the MASS simulation been available to forecasters, it would have provided excellent guidance for this case. MASS correctly forecast the location of secondary surface cyclogenesis to the lee of the Appalachian mountains at precisely the time it occurred. The model also predicted the potential for convection and an accurate forecast of increasing precipitation amounts in the Washington-Baltimore area in conjunction with an enhanced comma-shaped ascent maximum that was colocated well with observed precipitation reports

and satellite imagery. It also provided a good indicator of the rain-snow line near Washington, DC, where certain empirical arguments would have indicated that it lie further to the south across southeastern Virginia.

The MASS simulation of the severe weather outbreak across South and North Carolina on 28 March 1984 did not fare as well as the previous case. The model overforecast pressure falls and precipitation across the Middle Atlantic states prior to the outbreak of tornadoes, and underforecast the rapid deepening and movement of the intense low that was associated with the tornado outbreak in the southeastern United States. These errors may have detracted from the credibility of the forecast had it been available in real-time. Nevertheless, this simulation did indicate an increasing potential for convection in the Southeast during the afternoon and early evening of 28 March and correctly predicted the time and location of convective precipitation in North and South Carolina. The subtle, but nevertheless important, deficiencies in the 28 March forecast may be partially due to parameterizations of convection and a poor initial data base at 1200 GMT 28 March as numerous winds were missing near an intense upper-level jet streak prior to cyclone development. Sensitivity studies from other mesoscale model results have shown that the improper vertical distribution of latent heating (Anthes et al., 1983) and initial wind specifications (Chang et al., 1984) can seriously deteriorate the forecast.

The results from the 28 March model forecast again raise the issue whether the synoptic-scale operational data base is adequate and reliable on a day-to-day basis for mesoscale forecasting. There is growing evidence that the operational data base is "adequate" to produce a useful mesoscale forecast (Kaplan and Paine, 1972; Anthes, 1983; Koch, 1984; Koch et al.,

1984) in numerous situations where the synoptic-scale processes appear to drive the mesoscale circulation patterns. However, questions concerning the reliability of the rawinsonde network to capture key features in the initial temperature, wind, and moisture fields still persist. Furthermore, the theoretical framework for properly specifying mass and momentum balance constraints for initializing mesoscale models still needs to be properly resolved to prevent spurious wave activity (especially during the first 6 h of a simulation), which can significantly degrade the numerical forecast and mislead forecasters using the product.

Nevertheless, the results from this model, along with other recent mesoscale model studies (Anthes, 1983), indicate that there is a wealth of useful information inherent in mesoscale model simulations which could be available in real-time. These simulations, when combined with other data sources (e.g., radar and satellite), could prove to be a valuable aid to forecasters concerned with predicting significant weather events which are mesoscale in character.

Acknowledgements. We would like to thank the many individuals at the National Climatic Data Center in Asheville, NC, the National Severe Storms Forecast Center in Kansas City, MO, the National Meteorological Center in Camp Springs, MD, and Research and Data Systems, Inc. in Lanham, MD for providing data essential for the model comparison. Drs. Steven Koch and Daniel Keyser are acknowledged for their thorough reviews of the manuscript and suggestions. Mr. Lafayette Long and Ms. Kelly Wilson are recognized for their important technical support. We also thank Dr. James Dodge at

NASA Headquarters for continued financial support of MASS and
Mr. Norman Crabill for providing computer resources.

REFERENCES

- Anthes, R. A., 1977: A cumulus parameterization scheme utilizing a one-dimensional cloud model. Mon. Wea. Rev., 105, 270-286.
- _____, and D. Keyser, 1979: Tests of a fine-mesh model over Europe and the United States. Mon. Wea. Rev., 107, 963-984.
- _____, 1983: Regional models of the atmosphere in middle latitudes. Mon. Wea. Rev., 111, 1306-1335.
- _____, Y. Kuo, and J. R. Gyakum, 1983: Numerical simulation of a case of explosive marine cyclogenesis. Mon. Wea. Rev., 111, 1174-1188.
- Beebe, R. G., and F. C. Bates, 1955: A mechanism for assisting in the release of convective instability. Mon. Wea. Rev., 83, 1-10.
- Bhumralkar, C. M., 1975: Numerical experiments on the computation of ground surface temperature in an atmospheric general circulation model. J. Appl. Meteor., 14, 1246-1258.
- Browne, R. F., and R. J. Younkin, 1970: Some relationships between 850-millibar lows and heavy snow occurrences over the central and eastern United States. Mon. Wea. Rev., 98, 399-401.
- Chang, C. B., D. J. Perkey, and C. W. Kreitzberg, 1984: Impact of initial wind field on the forecast of a severe storm environment. Preprints, 10th Conf. Weather Forecasting and Analysis, Clearwater Beach, FL, June 25-29, Amer. Meteor. Soc., 513-520.
- Coats, G. D., V. C. Wong, J. W. Zack, and M. L. Kaplan, 1984: A numerical investigation of the effect of soil moisture gradients on the regional severe storm environment. Preprints, 10th Conf. Weather Forecasting

and Analysis, Clearwater Beach, FL, June 25-29, Amer. Meteor. Soc., 506-512.

Cram, J. M., and M. L. Kaplan, 1984: Variational assimilation of VAS data into the MASS model. Preprints, 10th Conf. Weather Forecasting and Analysis, Clearwater Beach, FL, June 25-29, Amer. Meteor. Soc., 373-379.

Cressman, G. P., 1959: An operational objective analysis system. Mon. Wea. Rev., 87, 367-381.

Deardorff, J. W., 1977: A parameterization of ground surface moisture content for use in atmospheric prediction models. J. Appl. Meteor., 16, 1182-1185.

Fritsch, J. M., and C. F. Chappell, 1980: Numerical prediction of convectively driven mesoscale pressure systems. Part I: Convective parameterization. J. Atmos. Sci., 37, 1722-1733.

Kaplan, M. L., and D. A. Paine, 1972: A macroscale-mesoscale numerical model of intense baroclinic development. J. Appl. Meteor., 11, 1224-1235.

_____, J. W. Zack, V. C. Wong, and J. J. Tuccillo, 1981: A mesoscale sixth-order numerical modelling system. Preprints, 5th Conf. Numerical Weather Prediction, Monterey, CA, November 2-6, Amer. Meteor. Soc., 143-149.

_____, J. W. Zack, V. C. Wong, and J. J. Tuccillo, 1982a: A sixth-order mesoscale atmospheric simulation system applicable to research and real-time forecasting problems. Symposium on Mesoscale Meteorology, CIMMS, Norman, OK, 38-84.

- _____, J. W. Zack, V. C. Wong, and J. J. Tuccillo, 1982b: Initial results from a mesoscale atmospheric simulation system and comparisons with the AVE-SESAME I data set. Mon. Wea. Rev., 110, 1564-1590.
- _____, J. W. Zack, V. C. Wong, and J. J. Tuccillo, 1982c: A mesoscale eighth-order numerical modelling system and the Red River tornado outbreak of 1979 (Part I - Model structure). Preprints, 12th Conf. Severe Local Storms, San Antonio, TX, January 11-15, Amer. Meteor. Soc., 546-553.
- _____, J. W. Zack, V. C. Wong, and J. J. Tuccillo, 1982d: A mesoscale eighth-order numerical modelling system and the Red River tornado outbreak of 1979 (Part II - Analysis and simulation of the tornado outbreak). Preprints, 12th Conf. Severe Local Storms, San Antonio, TX, January 11-15, Amer. Meteor. Soc., 554-555.
- _____, J. W. Zack, V. C. Wong, and G. D. Coats, 1984: The interactive role of subsynoptic scale jet streak and boundary layer processes in organizing an isolated convective complex. Accepted for publication in Mon. Wea. Rev.
- Koch, S. E., 1984: Application of a mesoscale atmospheric simulation system to the forecasting of intense mesoscale convective systems. Accepted for publication in Mon. Wea. Rev.
- _____, W. C. Skillman, P. J. Kocin, P. J. Wetzel, K. F. Brill, D. A. Keyser, and M. C. McCumber, 1984: Evaluation of the synoptic and mesoscale predictive capabilities of a mesoscale atmospheric simulation system. Accepted for publication in Mon. Wea. Rev.

- Lamb, H. H., 1955: Two-way relationship between the snow or ice limit and 1000-500 mb thicknesses in the overlying atmosphere. Quart. J. Roy. Meteor. Soc., 81, 172-189.
- Molinari, J., 1982: A method for calculating the effects of deep cumulus convection in numerical models. Mon. Wea. Rev., 110, 1527-1534.
- Spiegler, D. B., and G. E. Fisher, 1971: A snowfall prediction method for the Atlantic seaboard. Mon. Wea. Rev., 99, 311-325.
- Stage, S. A., and J. A. Businger, 1981: A model for entrainment into a cloud-topped marine boundary layer. Part I: Model description and application to a cold-air episode. J. Atmos. Sci., 38, 2213-2229.
- Uccellini, L. W., and D. R. Johnson, 1979: The coupling of upper- and lower-tropospheric jet streaks and implications for the development of severe convective storms. Mon. Wea. Rev., 107, 682-703.
- _____, R. A. Petersen, P. J. Kocin, M. L. Kaplan, J. W. Zack, and V. C. Wong, 1983: Mesoscale numerical simulations of the Presidents' Day cyclone: Impact of sensible and latent heating on the precyclogenetic environment. Preprints, 6th Conf. Numerical Weather Prediction, Omaha, NE, June 6-9, Amer. Meteor. Soc., 45-52.
- Wong, V. C., 1982: On the effect of the planetary boundary layer parameterizations in mesoscale numerical weather prediction. NATO Advanced Science Institute Series. Mesoscale Meteorology - Theory, Observations, and Models, Gascogne, France, 173-174.
- _____, J. W. Zack, M. L. Kaplan, and S. L. Chuang, 1983a: A numerical investigation of the effects of cloudiness on mesoscale atmospheric circulation. Preprints, 5th Conf. Atmospheric Radiation, Baltimore, MD, November 1-4, Amer. Meteor. Soc., 151-154.

- _____, J. W. Zack, M. L. Kaplan, and G. D. Coats, 1983b: A nested-grid limited area model for short term weather forecasting. Preprints, 6th Conf. Numerical Weather Prediction, Omaha, NE, June 6-9, Amer. Meteor. Soc., 9-15.
- Zack, J. W., 1981: A numerical/dynamical investigation of the role of subsynoptic inertial and isallobaric adjustments in organizing severe local storm ensembles. Ph.D. Thesis, Cornell University, Ithaca, NY, 300 pp.
- _____, V. C. Wong, M. L. Kaplan, and G. D. Coats, 1983: A nested-grid mesoscale numerical simulation of an isolated tornadic convective complex. Preprints, 13th Conf. Severe Local Storms, Tulsa, OK, October 17-20, Amer. Meteor. Soc., 336-341.
- _____, V. C. Wong, M. L. Kaplan, and G. D. Coats, 1984: A model-based investigation of the role of boundary layer fluxes and deep convective processes in the precipitation distribution of East Coast cyclones. Preprints, 10th Conf. Weather Forecasting and Analysis, Clearwater Beach, FL, June 25-29, Amer. Meteor. Soc., 588-595.